Marine and Petroleum Geology 103 (2019) 87–113

Contents lists available at ScienceDirect

Marine and Petroleum Geology

journal homepage: www.elsevier.com/locate/marpetgeo

Research paper

The influence of base-salt relief, rift topography and regional events on salt tectonics offshore Morocco

Leonardo M. Pichel[a,b,*], Mads Huuse[a], Jonathan Redfern[a,b], Emma Finch[a]

[a] School of Earth and Environmental Sciences, University of Manchester, Oxford Road, Manchester, M13 9PL, UK
[b] North Africa Research Group, University of Manchester, Oxford Road, Manchester, M13 9PL, UK

ARTICLE INFO

Keywords:
Salt tectonics
Diapirism
Allochthonous salt
Salt sheets
Minibasin
Base-salt relief
Ramp-syncline basins
Morocco

ABSTRACT

This study integrates borehole-calibrated 2D and 3D seismic interpretation with numerical models to provide a regional analysis of the complex salt tectonics offshore central Morocco. We investigate the mechanisms controlling along-margin structural variations, the effects of thick-skinned shortening and the sequential evolution of allochthonous sheets. Additionally, we analyse how base-salt relief generated complex flow kinematics and alternation of extensional and contractional domains by causing flux variations at both autochthonous and allochthonous salt levels. The area is divided into three structural provinces, with the central, Essaouira segment, having greater downdip translation, structural complexity and volume of allochthonous salt, which suggests the salt was originally thicker and better connected across multiple syn-rift structures. The southern segment, Agadir, is dominated by up-right squeezed diapirs formed by early load-driven rise and late shortening; limited salt and overburden translation and no allochthonous sheets. The northern segment, Safi, is narrower and has a smaller number of salt structures that were affected by abrupt translation due to steep detachment gradient. Late, oblique thick-skinned shortening generated contractional structures in the entire salt basin, which are most prominently developed in Essaouira due to a favourably-oriented NW-SE syn-rift structure, the Talfeney Accommodation Zone. Allochthonous salt sheets formed during four phases from the Albian, Late Cretaceous, Paleocene to Oligo-Miocene by two main mechanisms: contraction and basinward salt expulsion. This work improves understanding of the structural configuration along the Moroccan margin guiding the identification of potential sub-salt plays and contributing to a better comprehension of salt-related deformation along rifted passive margins worldwide.

1. Introduction

The Moroccan Atlantic margin contains the longest (c. 1000 km) and widest (50–150 km) salt basin of NW Africa (Tari et al., 2003, 2017; Davison, 2005). The basin is characterized by prominent along-strike variations in salt-related structural styles and basin geometry (Fig. 1a), being divided into five distinct structural domains (Tari et al., 2003, 2012). Salt was deposited from the Late Triassic to early Jurassic during the Early Jurassic break-up of the African and North American plates (Tari et al., 2003; Davison, 2005). Similar to the conjugate margin offshore Nova Scotia (Albertz et al., 2010; Deptuck and Kendell, 2017) and other Atlantic margin basins (e.g. Parentis Basin, Ferrer et al., 2012), the salt in Morocco is interpreted to be late syn-rift (Tari et al., 2003, 2012; Tari and Jabour, 2013; Davison, 2005). The syn-rift deposition resulted in thicker salt in the hangingwall of predominantly NNE-NE half-grabens and thinner to non-existent salt over their footwalls; ultimately producing a discontinuous salt interval across the basin (Tari et al., 2003; Tari and Jabour, 2013). Owing to complex salt deformation, its syn-rift nature and the lack of deep-well penetrations of the autochthonous salt, estimates of the original salt thickness are uncertain, ranging between a few hundred meters (Tari et al., 2017) to over 1.5 km (Davison, 2005) in their thickest portions.

Petroleum systems have been documented onshore Morocco, in the Essaouira-Agadir Basin (Jabour et al., 2004: Tari and Jabour, 2013) but the offshore part of the margin remains relatively sparsely explored, with no commercial discoveries to date. On the conjugate margin in Nova Scotia, however, a number of fields have been discovered along the shelf and deep-water exploration is ongoing (Tari et al., 2012). Many salt-related plays have been proposed (Tari et al., 2012; Tari and Jabour, 2013) but most of them remain untested, suggesting there may be still untouched exploration potential along the margin (Fig. 1b). Despite the lack of proven reservoir-quality sediments in the Upper

* Corresponding author. School of Earth and Environmental Sciences, University of Manchester, Oxford Road, Manchester, M13 9PL, UK.
E-mail address: leonardo.munizpichel@manchester.ac.uk (L.M. Pichel).

https://doi.org/10.1016/j.marpetgeo.2019.02.007
Received 27 August 2018; Received in revised form 4 February 2019; Accepted 5 February 2019
Available online 13 February 2019
0264-8172/

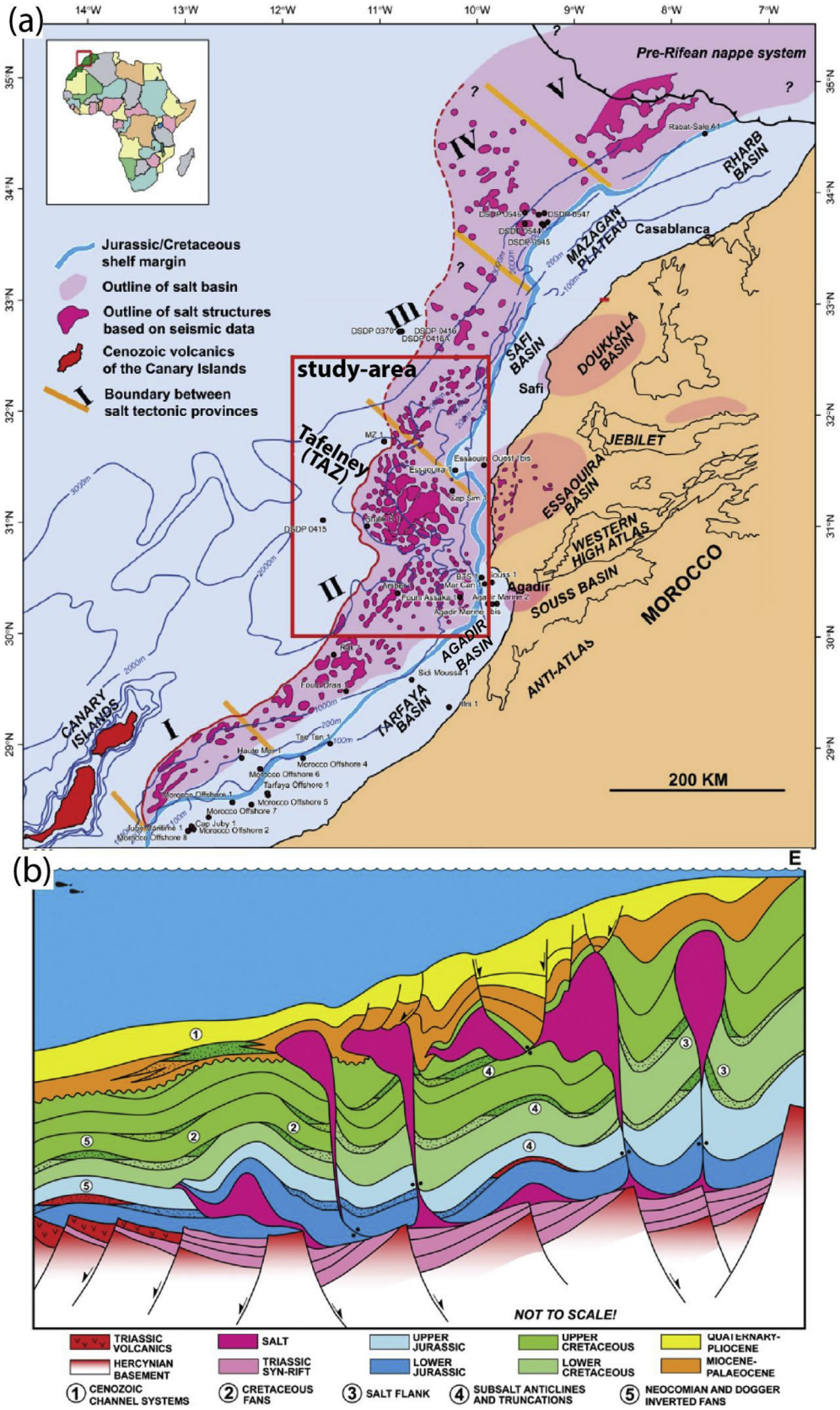

Fig. 1. (a) Regional map showing the outline of the Moroccan salt basin and its five main salt-related structural domains along the Moroccan margin (adapted from Tari and Jabour, 2013). (b) Schematic summary diagram of potential hydrocarbon plays associated with salt structures along the margin, most of which remain largely untested (from Tari and Jabour, 2013).

Cretaceous and Cenozoic targets, many regional elements point to the presence of turbiditic deepwater fans in the Lower Cretaceous and Middle Jurassic (Lancelot and Winterer, 1980; Tari et al., 2012). More recent studies also document the existence of fluvial feeder systems that could be the source for deepwater fans in the Lower Cretaceous (Luber, 2017; Luber et al., 2019). Due to the long-lived and dynamic salt deformation (Hafid et al., 2000; Tari et al., 2003, 2012; Davison, 2005), salt has acted as a strong control in the distribution of depocentres and sediment fairways across the slope and deep-basin, generating potential hydrocarbon traps and migration pathways. Thus, understanding the controls, timing, kinematics and distribution of salt-related structures is critical to de-risk deep-water hydrocarbon exploration in the area.

As a consequence of the limited availability of high-resolution seismic data and deep-water wells, salt tectonics offshore Morocco and in most syn-rift salt basins (Tari et al., 2003; Davison, 2005), is relatively less well understood compared with their post-rift counterparts in the Gulf of Mexico and South Atlantic (Hudec and Jackson., 2004; Rowan et al., 2004; Davison et al., 2012; Quirk et al., 2012; Hudec et al., 2013; Peel, 2014b; Rowan, 2014, 2018; Jackson et al., 2015a,b). The variety of salt-related structural styles and interaction with complex basin geometries make Morocco one of the most interesting places to study salt tectonics, especially in light of recent modelling advances and novel aspects of effects of pre-salt relief on salt flow (Dooley and Hudec, 2016; Dooley et al., 2016, 2018; Ferrer et al., 2017; Pichel et al., 2018a, b), which are particularly relevant for syn-rift salt (Jackson and Hudec, 2017).

Previous studies provided a regional analysis of salt tectonics offshore Morocco, describing significant along-strike variations in basin geometry and salt-related structures (Fig. 1) (Davison, 2005; Tari and Jabour, 2013; Tari et al., 2003, 2012). In this study, we expand on them by integrating new seismic (2D and 3D) and well data with both numerical and kinematic models to: 1) test earlier concepts, 2) investigate the mechanisms controlling different salt-related geometries and kinematics along the margin; 3) analyse the effects of base-salt topography and regional tectonic events on salt deformation; and 4) evaluate the timing and generation of allochthonous salt and their potential effects on paleo-bathymetry. The results offer a better comprehension of salt tectonics offshore Morocco, being also relevant for other syn-rift salt basins worldwide. From an applied perspective, this contributes to the regional knowledge of the distribution of potential traps and reservoirs in the deepest and more commercially interesting supra-salt intervals (i.e. Jurassic and Lower Cretaceous, Tari et al., 2012) along the margin.

2. Tectono-stratigraphic framework

The evolution of the Moroccan continental margin started with Triassic rifting associated with opening of the Central Atlantic Ocean and deposition of fluvial red beds and evaporites intercalated with basaltic magma in NNE-SSW to NE-SW half-grabens (Hafid et al., 2000, 2006; Le Roy and Piqué, 2001; Davison, 2005; Tari et al., 2003, 2012; Tari and Jabour, 2013). A NW-SE syn-rift high, referred to as the Tafelney Accommodation Zone (TAZ), marks a switch in syn-rift fault polarity from NW-dipping faults to the south to SE-dipping faults to the north (Tari and Molnar, 2005; Tari et al., 2012).

Break-up and onset of continental drift occurred during the Early Jurassic, with thermally-induced subsidence and eustatic sea-level rise resulting in marine conditions and widespread carbonate sedimentation during most of the remaining Jurassic, with interbedded siliciclastic deposition related to a basin-wide regression (Davison, 2005; Tari et al., 2012; Tari and Jabour, 2013). An Early Cretaceous sea-level rise drowned the carbonate platform and marked a change to siliciclastic sedimentation (Tari et al., 2012; Tari and Jabour, 2013; Luber et al., 2019) (Fig. 2). Carbonate sedimentation returned briefly during the Albian; and throughout the remaining Late Cretaceous and Cenozoic sedimentation was dominated by mudstones and calciturbidites in deep-waters, with apparently very little influx of sands (Tari et al., 2012). The most proximal regions were affected by several episodes of uplift and erosion due to regional compressional tectonics associated with the Atlasic Orogeny, following the collision of Africa with the Iberia Plate and epeirogenic uplift of Africa from the Senonian to recent (Fig. 2) (Hafid et al., 2000, 2006, Davison, 2005; Frizon de Lamotte et al., 2009; Tari and Jabour, 2013). Many authors have argued that thick-skinned compressional events had an influence on the overall structural style of the basin, controlling both onshore (Hafid et al., 2000, 2006; Saura et al., 2014; Vergés et al., 2017) and offshore salt tectonics (Tari et al., 2003, 2012) by progressively tilting the margin and reactivating previous salt bodies.

Due to the dearth of deep-water wells, the older stratigraphy of the margin is still not well understood, relying on projected information from outcrops onshore Morocco and on Fuerteventura which provide analogues for this deepwater succession (Tari et al., 2012). In Fuerteventura, Jurassic deepwater carbonates directly overly oceanic crust, marking the onset of the drift phase (Aalenian-Bajocian) and being age-equivalent to the prolific carbonate platform inboard (Jansa and Wiedmann, 1982; Steiner et al., 1998; Davison, 2005; Tari et al., 2012). These carbonates are overlain by Jurassic pelagic mudstones, siliclastics turbidites and calciturbidites and Berriasian-Barremian siliciclastics (Tari et al., 2012). Additionally, a series of mass-transport complexes are documented in a seismic-based study (Dunlap et al., 2010), and occur predominantly in the Upper Cretaceous section due to catastrophic failure of the central portion of the margin in the Essaouira Basin.

3. Methods

This study is based on the integration of zero-phase, time-migrated 2D regional seismic profiles and 3D seismic data covering c. 2500 km^2 offshore the Essaouira-Agadir Basin with six offshore wells and numerical models to analyse the salt tectonics along the margin (Fig. 3). Seismic displays follow the Society of Economic Geologists (SEG) normal polarity, where an increase in acoustic impedance with depth is represented by a positive reflection event (red on seismic sections) and a decrease in acoustic impedance by a negative event (blue on seismic sections) (Brown, 2011). 3D and 2D seismic profiles are from different surveys, having variable frequency and resolution. The dominant frequency for the Jurassic varies between 22 and 28 Hz, for the Lower and Upper Cretaceous, it varies between 30-35 and 35–38 Hz respectively; and between 40 and 50 Hz for the Cenozoic. Based on calibration with sonic-logs from well-ties, the mean interval velocities for these successions are around 2300 m/s for the Cenozoic, 2550 m/s and 2700 m/s for the Upper and Lower Cretaceous respectively. As the Jurassic was only penetrated by two wells on the shelf (Essaouira 1 and Essaouira W-1, Fig. 3), estimates of deep-water facies velocities are less certain. However, as the Jurassic consists of a carbonate-dominated succession on the shelf (Hafid et al., 2000, 2006; Tari et al., 2012), we infer a marl-dominated slope and deep-basin section, with velocities ranging from 4000 to 4400 m/s. These values yield an approximate range of vertical resolution of 12–15 m for the Cenozoic, 16–18 m for Upper Cretaceous, 19–22 m for the Lower Cretaceous and of 36–50 m for the Jurassic. The interpretation of key stratigraphic horizons is based on calibration to two deepwater wells (Shark B-01 and Amber 01) and four wells at the shelf (Essaouira 1, Essaouira W-1, Cap Sim 01 and BTS-01), seismic facies and structural pattern correlations (Fig. 4).

4. Results

4.1. Seismic facies and geometry of key stratigraphic intervals

The Jurassic is characterized by a lower section dominated by moderate amplitude and moderate-low continuity reflections with occasional, local high amplitude events, passing upwards to moderate-high continuity, low amplitude reflections (Fig. 4). It displays marked

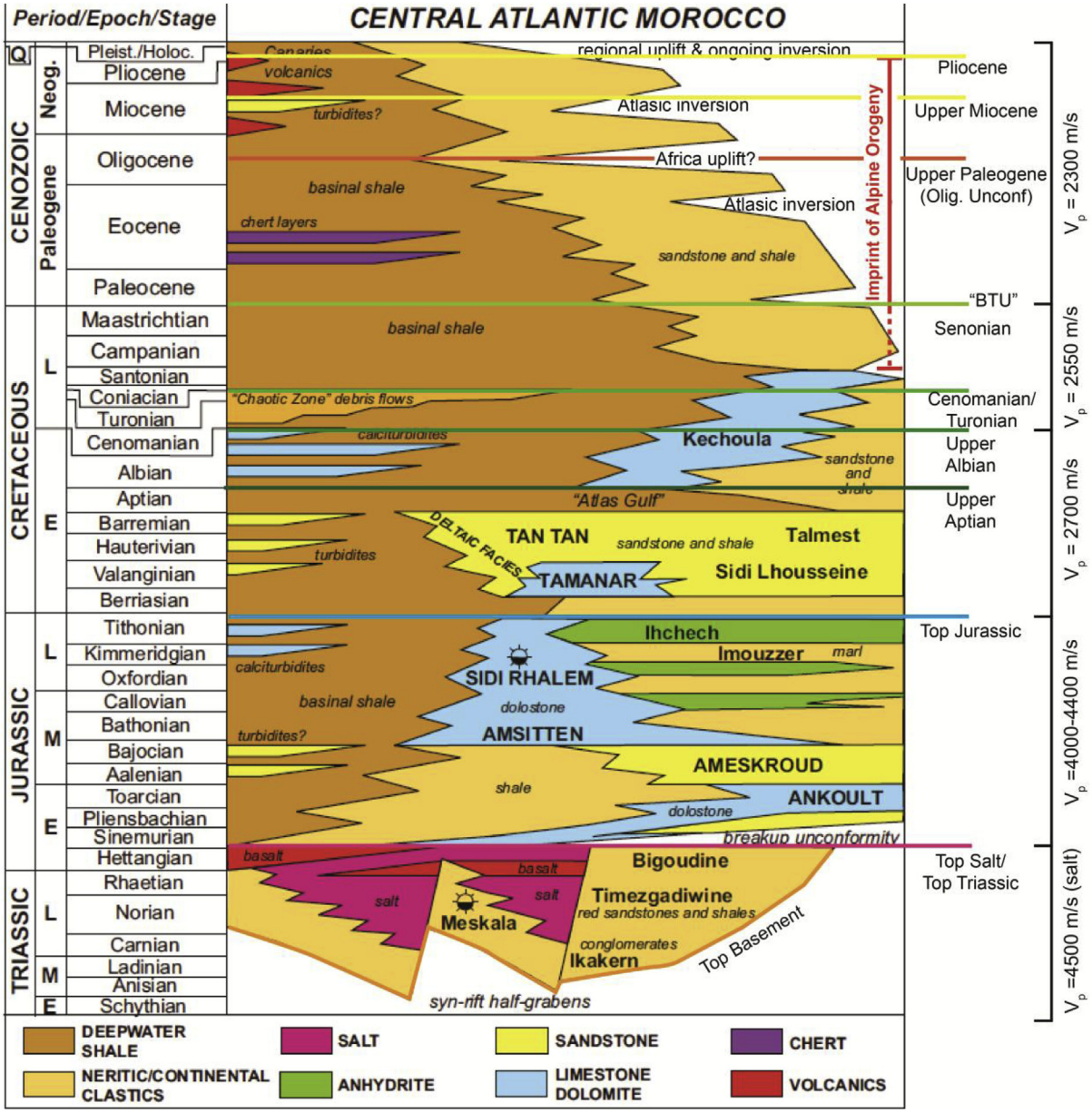

Fig. 2. West to East stratigraphic column of Central Atlantic on- and offshore Morocco with the seismic horizons mapped and their respective mean interval velocities highlighted (adapted from Tari and Jabour, 2013). The timing of imprint of Alpine/Atlas orogeny is also annotated.

thickness variations across the basin, suggesting strong control on accommodation by salt movement (Figs. 4–8). Its base is defined by a transition from broadly parallel and continuous reflections within the Jurassic to chaotic or wedge-shaped intervals that represent basement and Triassic syn-rift strata respectively (Fig. 4). The top Jurassic is defined by a high-amplitude positive event that is interpreted to mark the transition from a carbonate-rich section to deep-water clastics of Lower Cretaceous age (Fig. 4) (Tari et al., 2012; Tari et al., 2017).

The Lower Cretaceous (Barremian-Aptian, Fig. 4) is characterized by moderate-high continuity and moderate amplitude reflections, transitioning upward to a low amplitude and high-continuity interval delimited at the top by a high-amplitude positive event. The oldest interval penetrated by deep-water wells in the study area (Shark B-1, Cap-Sim 1 and Amber 1, Figs. 3–4) is Albian in age (Tari et al., 2012), although more recent wells outside the area or not available in this study are reported to have penetrated Aptian (FA-1), Jurassic and possibly Triassic deep-water successions (FD-1 and MZ-1) (W. Leslie, pers. comm. 2018). The Albian interval is broadly isopachous over most of the basin, suggesting a period of decreased salt movement, being dominantly represented by low amplitude and low-continuity seismic facies (Fig. 4). This interval is defined at the top by a positive bright event with moderate continuity that marks an abrupt change to mass-transport complexes characteristic of the Cenomanian (MTCs, Fig. 4) (Dunlap et al., 2010). The Cenomanian presents profound thickness variations and multiple local unconformities over most of the study area (central and northern segments), being characterized by chaotic-to low continuity seismic facies with intermediate high-amplitude and moderate continuity events (Fig. 4). Its top is defined by a moderate-high amplitude positive event and a transition to highly continuous, moderate-high amplitude reflections of the remaining Upper Cretaceous, herein referred to as Senonian for simplicity (Fig. 4) (c.f. Tari and Jabour, 2013; Tari et al., 2017).

The transition to the Cenozoic is marked by a regional erosional unconformity, the Base Cenozoic Unconformity, also known in the literature as the Base Tertiary Unconformity (BTU, Neumaier et al., 2016) (Fig. 4), which is overlain by highly continuous and variable amplitude

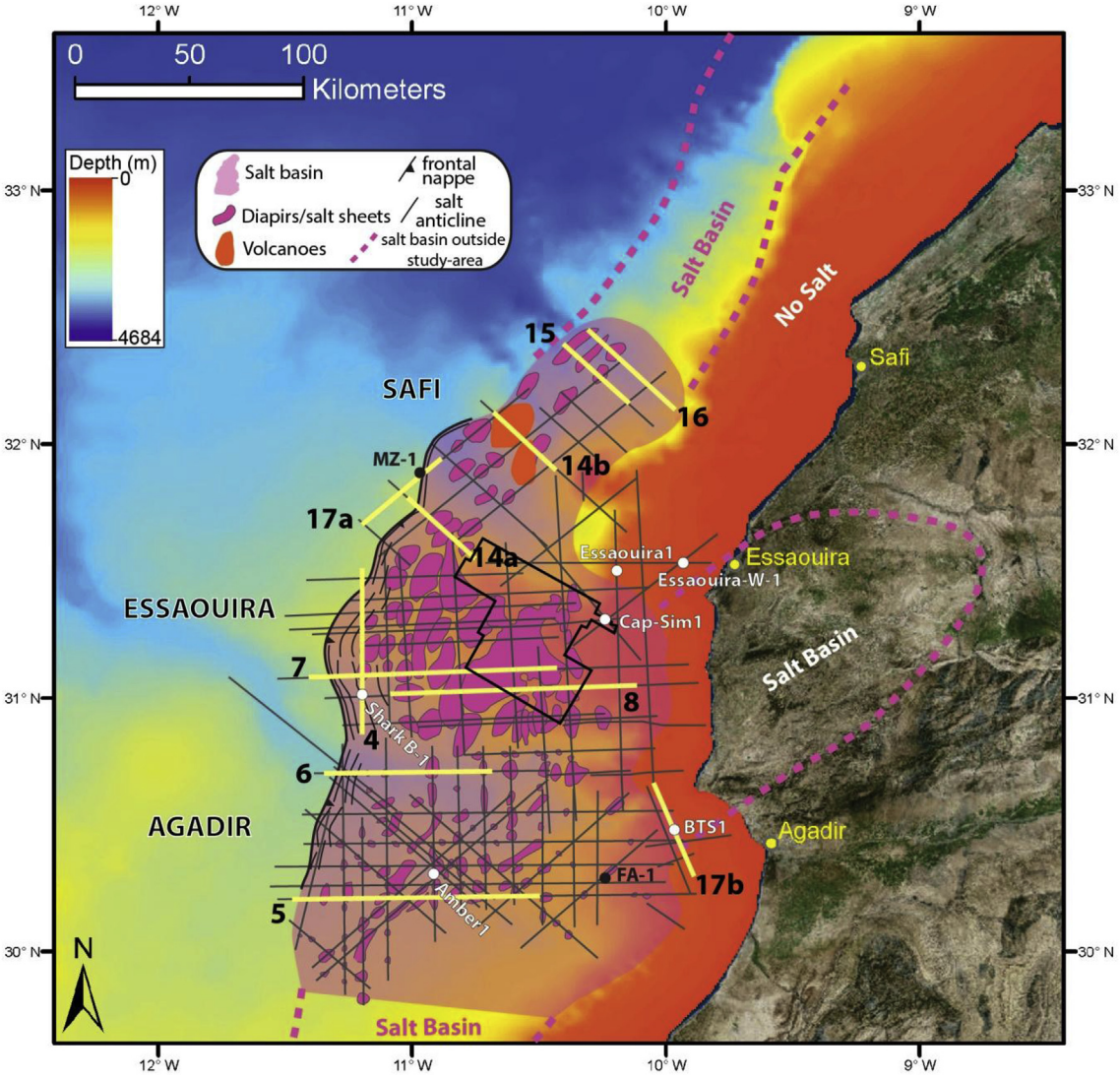

Fig. 3. Study-area map with the outline of the salt basin and main salt structures overlying the present-day bathymetry. The study focuses on three salt provinces that are, from south to north: Agadir, Essaouira and Safi. 2D seismic sections are represented by grey lines, wells in white (used in this study) and black (not available) dots, and outline of the 3D survey in the black polygon. Seismic profiles presented in this study are in yellow and numbered according to their respective figure. Onshore satellite image from the ArcMap Online World Imagery layer and the bathymetry from the General Bathymetric Chart of the Oceans (cf. Weatherall et al., 2015). (For interpretation of the references to colour in this figure legend, the reader is referred to the Web version of this article.)

facies of Paleogene age. This interval also displays prominent thickness variations and a number of local unconformities can be determined. The top of this interval is defined by an Early Oligocene unconformity (Fig. 4). The remaining Cenozoic is also marked by profound thickness changes intercalated with almost isopachous intervals, both of which display high-moderate amplitude and high-continuity seismic facies. Middle Miocene and Middle Pliocene unconformities mark renewed pulses of regional tectonics linked to the Atlas Orogeny (Tari et al., 2012, 2017).

Autochthonous and allochthonous salt intervals were defined mainly based on geometries and lateral and/or vertical transition from layered, highly reflective intervals, interpreted to be bedded clastic or carbonate sediments, to chaotic-transparent facies associated with salt. Gently-dipping allochthonous top-salt was generally identified as a positive (red) bright event, especially when in contact with the Upper Cretaceous-Cenozoic succession and base-salt as a negative (blue) event (Figs. 4–7). The amplitude of these horizons, however, varies considerably according to the juxtaposed units.

The Identification of feeders associated with allochthonous salt was based primarily on the interpretation of higher resolution 3D seismic data and generation of structure maps of the base and top allochthonous canopy. The presence of feeders in cross-section is then inferred based on the identification of truncations and abrupt lateral changes in geometry aligned with base-allochthonous-salt lows and top-autochthonous-salt highs (Figs. 4–9). In cases where feeders are dipping more gently, they are defined by bright, variably-dipping positive reflections that increase the confidence of their interpretation (Figs. 7–9). The identification of feeders allowed recognition of individual allochthonous salt sheets that merged to form large canopies (Figs. 7–9). This was coupled with the chronostratigraphic framework obtained from well-seismic ties and mapping of key horizons (Fig. 4) to provide improved estimates on the timing and mechanisms of emplacement of allochthonous salt along the margin. The timing of emplacement was defined by reasonably confident age estimates of the youngest strata underlying the salt sheets.

The base Triassic could be defined locally and is characterised by downwards and/or lateral abrupt transitions from gently-dipping, moderately continuous seismic facies that define typical syn-rift wedge intervals, to chaotic/transparent facies below, interpreted to be the high-velocity basement. This observation provided local constraints of

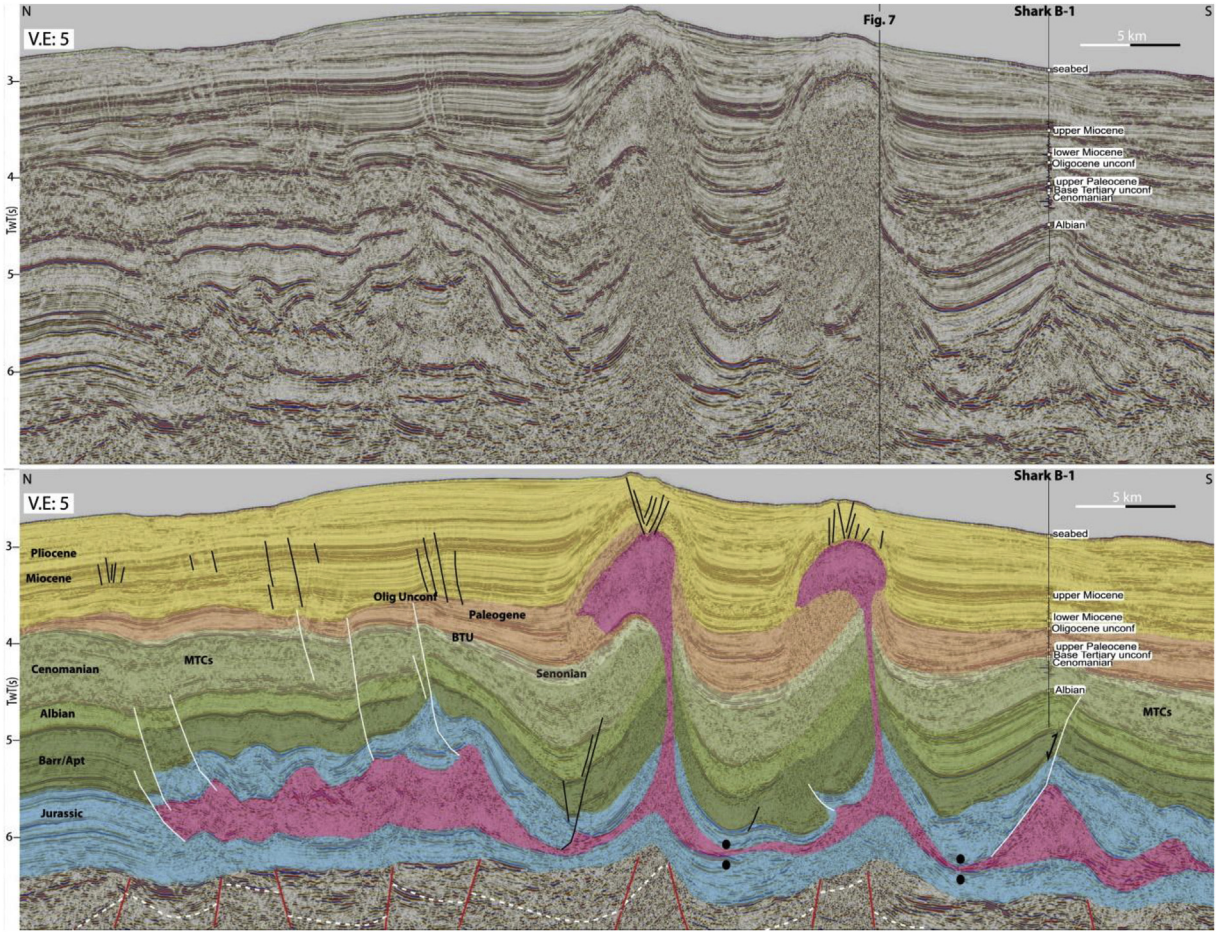

Fig. 4. Uninterpreted and interpreted strike-oriented seismic section over the downdip edge of the salt basin offshore Essaouira and deep-water Shark B-1 well penetrating Upper Albian interval at the crest of a salt-cored anticline (Tari et al., 2012). This anticline formed by a combination of extension and inversion over the salt nappe. Sub-vertical squeezed feeders associated with inflated salt tongues having minor sea-floor expression are interpreted not to be welded due to current activity and uplift of a thick overburden. The section also shows folding and thrusting related to advance of salt nappe over syn-kinematic Jurassic sediments and a zone of folding and uplift north of the salt basin associated with thick-skinned contraction. Uninterpreted section exemplifies the main seismic facies associated with main stratigraphic interval interpreted in this study. Vertical Exaggeration is c. 5-fold based on an average velocity of 4000 m/s.

syn-rift geometries and allowed identification of basement faults in areas where imaging is less affected by large volumes of salt (Figs. 4–6).

Correlation of Mesozoic-Cenozoic intervals across the complex salt structures and minibasins is challenging in parts of the dataset, especially for the deeper and consequently lower resolution intervals, and sections below thick allochthonous salt (Figs. 4–8). Nevertheless, interpretation in areas of higher confidence could be extended out- and/or inboard of the salt basin and areas with a stronger imprint of salt movement. This was performed by initially following seismic and structural trends of the main reflections within minibasins and identifying seismic artefacts related to multiples and velocity pull-ups (Jones and Davison, 2014); and, subsequently, estimating ages based on regional analysis and thickness patterns (Figs. 4–6). Nonetheless, a degree of uncertainty exists for the deeper (Jurassic-Albian) and, therefore, more deformed intervals in areas far from wells and/or below allochthonous salt sheets.

4.2. Salt-related structures and along-strike variation across the margin

The Moroccan Atlantic margin is characterized by a complex pattern of salt walls, diapirs and allochthonous salt sheets with prominent along-strike variation (Tari et al., 2003, 2012; 2017; Tari and Jabour, 2013) comparable to its conjugate margin in Nova Scotia (Ings and Shimeld, 2006; Albertz et al., 2010; Deptuck and Kendell, 2017). Five different salt tectonics domains were defined by Tari et al. (2012) and Tari and Jabour (2013) (Fig. 1).

The southernmost, Segment I (Cap Juby area), is characterized by few and simple structures represented by salt pillows and up-right diapiric salt walls, downdip of the large Jurassic shelf (Fig. 1). Northwards, Segment II (Tarfaya and Agadir Basins), comprises a large number of salt walls and stocks, a few of which are associated with minor salt tongues and are described as being mainly driven by sedimentary loading during the Cenozoic (Tari et al., 2003, 2012; Tari and Jabour, 2013) (Fig. 1a). The north of Segment II (Tafelney Plateau, Essaouira Basin) is defined as the salt-richest portion of the margin with a larger number of structures and most complex salt tectonics characterized by allochthonous salt sheets and an outboard salt nappe and fold-thrust belt (Tari and Jabour, 2013). Segment III (Safi) contains fewer salt structures and only small (c. 10–20 km^2) allochthonous salt bodies, probably due to a smaller original volume of salt (Tari et al., 2012). The northernmost segments contain simpler salt tectonic styles, characterized by a large number of diapirs in Segment IV, with a few long (c. 100 km) salt walls in Segment V (Fig. 1a) (Tari et al., 2012; Tari and Jabour, 2013).

Similar to the conjugate margin (Adam and Krézsek, 2012; Deptuck and Kendell, 2017), the syn-rift nature of the salt has been demonstrated to be an important factor on the evolution of Atlantic Morocco, controlling original along-strike thickness variations (salt-rich and salt-poor segments, c.f. Tari et al., 2003, 2012; Tari and Jabour, 2013) and also limiting salt-detached translation (Tari and Jabour, 2013).

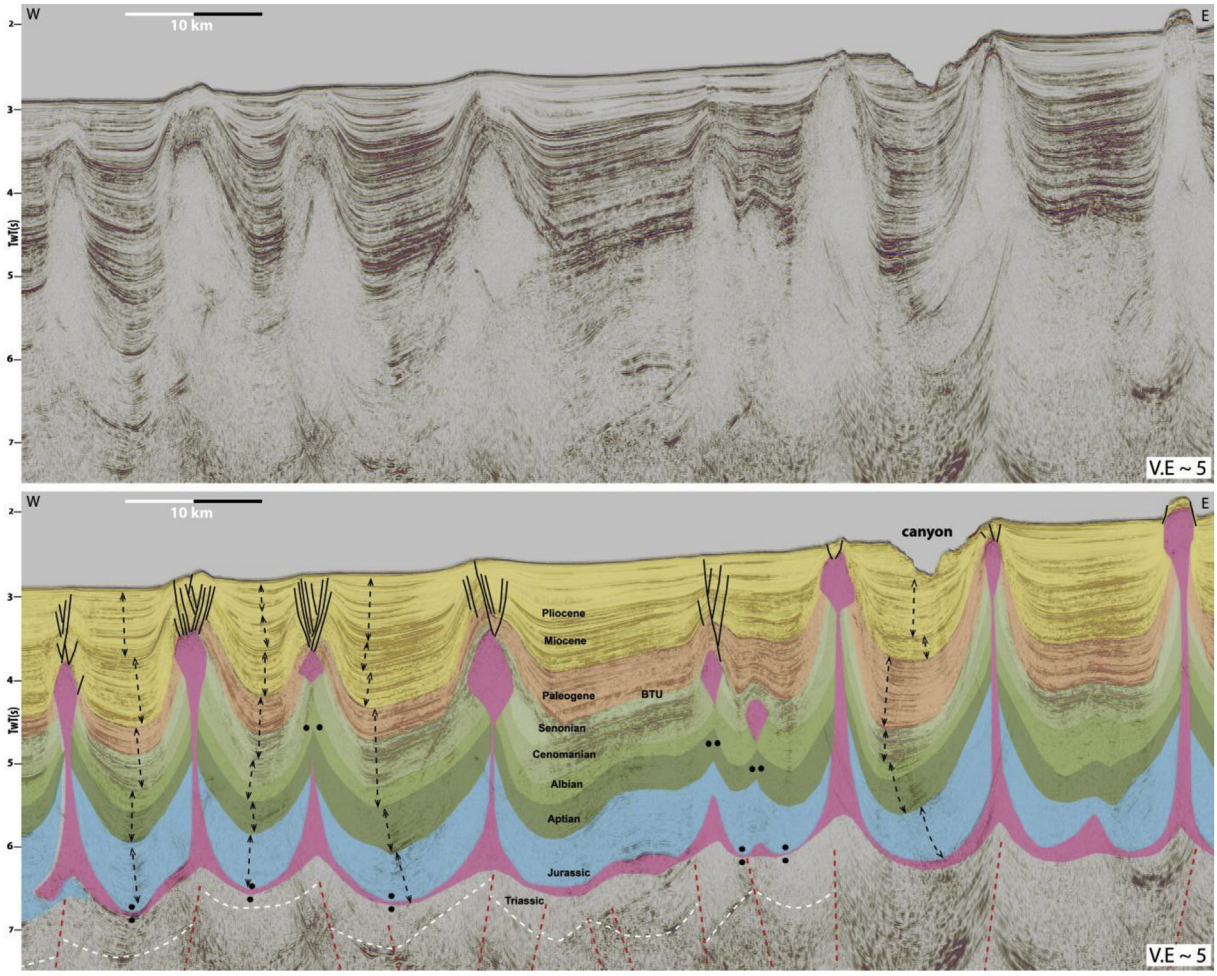

Fig. 5. Uninterpreted and interpreted regional seismic section at the southern portion of Agadir Basin showing tall, up-right, highly-squeezed and broadly symmetric diapirs, some of which forming tear-drop structures and others with sea-floor expression. Minibasins present strong thickness variations from Jurassic-Lower Cretaceous and Paleogene-Miocene indicating the main period of growth, mostly associated with regional shortening as evidenced by an abrupt shift of depocentres (black dashed lines). Sub-salt dashed-lines are used for faults (red) and the base-Triassic horizon (white), which are subject to uncertainties due to typical sub-salt imaging issues but can be inferred based on a combination of supra-salt geometries and sub-salt seismic facies variations and truncations. Two types of faults occur at the crest of diapirs, keystone and flap faults (c.f. Rowan et al., 1999), which indicate outer-arc extension, roof uplift and contraction during the Cenozoic. Vertical Exxageration is c. 5-fold based on an average velocity of 4000 m/s. (For interpretation of the references to colour in this figure legend, the reader is referred to the Web version of this article.)

Nonetheless, the effects of pre-salt rift topography and associated salt thickness variations on supra-salt kinematics and structural styles; combined with the influence of margin configuration, base-salt relief and late tectonic events on the generation of allochthonous salt along the margin have not yet been addressed in detail. This paper, therefore, focuses on segments II-III of the original division of Tari et al. (2012) (Fig. 1), subdividing them into 3 segments: the (1) Agadir; (2) Essaouira and (3) Safi Basins (Fig. 3) to investigate these issues.

4.2.1. Agadir Basin

This segment has the thickest overburden at c. 7 km, and deepest autochthonous salt (c. 9–10 km depth below sea surface) of the entire study-area (Fig. 5). The area is characterized by tall (c. 4–6 km), up-right diapirs with thin (< 400 m wide) to welded sub-vertical stems and, predominantly, broadly symmetric salt bulbs up to 2 km wide, defining classic tear-drop diapirs (Fig. 5). Despite the 2D nature of the dataset in this segment, certain structures can be followed in multiple sections along-strike and are characterized as 5–10 km long walls trending predominantly NE-SW. The majority of diapirs, however, can be described as salt stocks having an axial ratio of less than two (c.f. Jackson and Hudec, 2017) (Fig. 3).

These diapirs are surrounded by 5–10 km wide minibasins, 3–7 km thick, that are apparently welded or occur above thin (c. 200 m) autochthonous salt (Fig. 5). These minibasins exhibit pronounced thickness variations in the Middle Jurassic to Early Cretaceous interval, which are directly and often abruptly truncated against the diapiric stems. This indicates early passive rise driven by differential sedimentary loading and salt expulsion below subsiding minibasins (*sensu* Hudec et al., 2009, Peel, 2014a). Some of the Jurassic-Lower Cretaceous depocentres present landward-dipping depositional axial traces (dashed black line, Fig. 5) that may indicate an early phase of expulsion rollover. A brief precursor phase of reactive rise is likely to have occurred in the Early-Middle Jurassic, as salt had been deposited at the end of the rift stage and, thus, syn-extension (*sensu* Rowan, 2014; Jackson and Hudec, 2017), but this is overprinted by a long-lived, multiphase growth (Tari and Jabour, 2013; Tari et al., 2017).

Thickness variations within minibasins and, consequently, the record of salt activity generally decrease during the Albian-Cenomanian and most diapirs become partially buried by Senonian-Paleocene strata (Figs. 5 and 6). The diapirs, however, push and uplift a relatively thick (up to 1.5 km), isopachous roof that is onlapped by Miocene-Pliocene strata exhibiting significant thickness variations and indicating diapirism was rejuvenated by renewed pulses of active rise during this time (Fig. 5). Keystone and flap faults (*sensu* Rowan et al., 1999) develop at

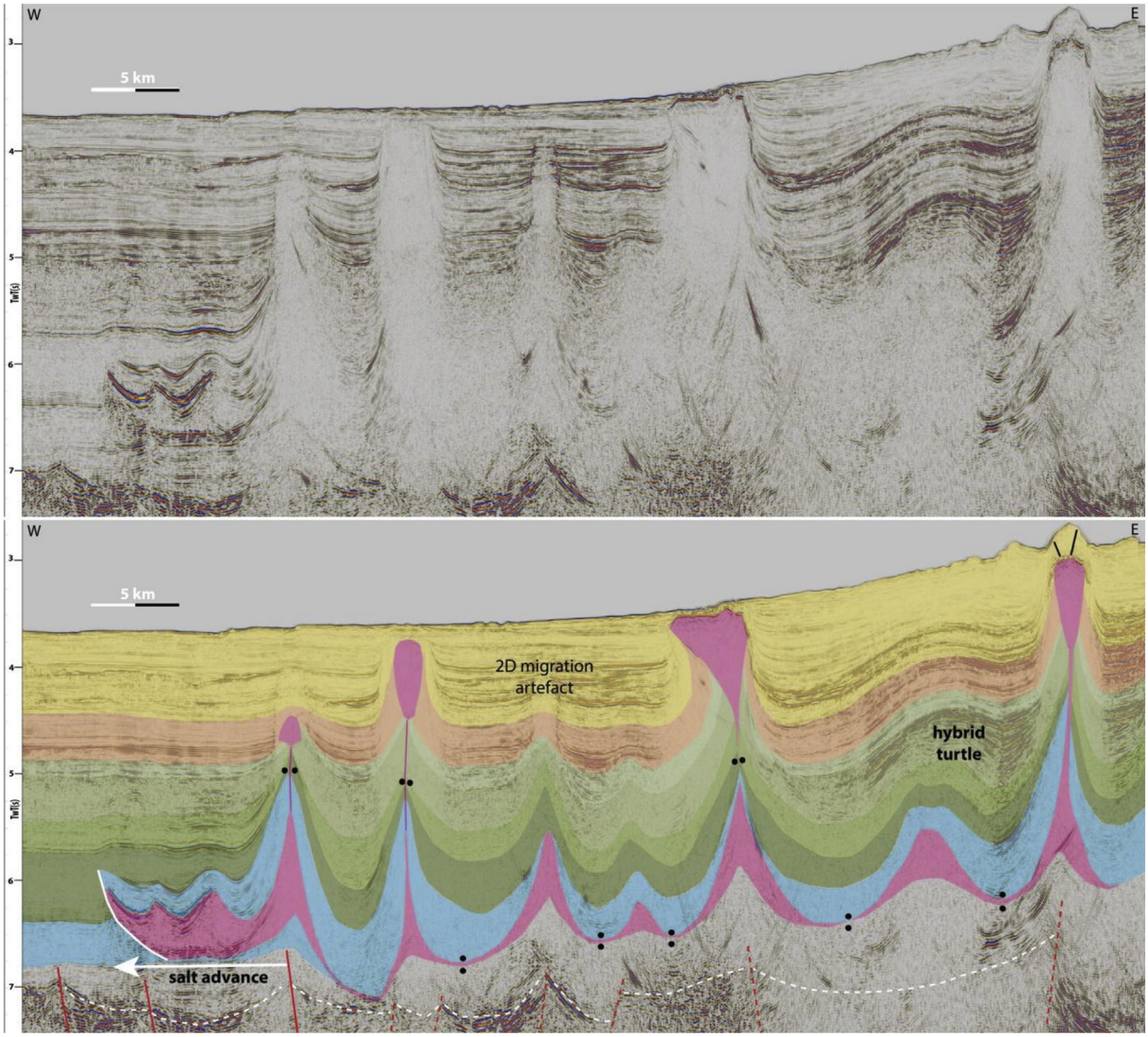

Fig. 6. Uninterpreted and interpreted regional seismic section north of Agadir, near the transition to Essaouira showing an 8 km wide salt nappe recording frontal advance, passing updip to up-right tear-drop to a sub-vertical squeezed feeder and inflated salt tongue and another up-right squeezed diapir with sea-floor expression further updip. Hybrid turtle anticline forms between the latter due to a combination of salt subsidence and translation over a large pre-salt graben. Sub-salt dashed-lines are used for faults (red) and the base-Triassic horizon (white), which are subject to uncertainties due to typical sub-salt imaging issues but can be inferred based on a combination of supra-salt geometries and sub-salt seismic facies variations and truncations. Vertical Exxageration is c. 5-fold based on an average velocity of 4000 m/s. (For interpretation of the references to colour in this figure legend, the reader is referred to the Web version of this article.)

their crests due to outer-arc extension and, combined with sub-vertical squeezed stems and abrupt shifts of the depositional axial-traces within minibasins (Fig. 5) (c.f. Hudec et al., 2009), indicate that active rise was driven by shortening. The smaller tear-drop diapirs become dormant by the Pliocene, but most structures present sea-floor expression denoting ongoing activity (Figs. 5 and 6).

In the southernmost portion of this segment, the absence of a salt nappe at the frontal edge of the salt basin and the predominantly vertical salt structures suggest no significant basinward translation (Fig. 5). Salt and overburden translation due to basinward gliding increase progressively northwards towards Essaouira, but is relatively minor (< 10 km) as shown by the appearance of a 5–9 km wide, c. 1.5 km thick, sub-horizontal salt nappe and symmetric fold-belt at its northern limit with the Essaouira segment (Fig. 6). Diapir spacing is c. 8–10 km downdip, and most diapirs, especially the largest of them, appear to be, at present, above or near the footwall crest of syn-rift faults in areas where these can be estimated (Figs. 5 and 6).

4.2.2. Essaouira Basin

The central segment, the offshore Essaouira Basin, also referred as Tafelney Plateau (c.f. Tari and Jabour, 2013), has a strikingly different structural style, being characterized by a large number of allochthonous salt bodies, seaward-verging diapirs and salt tongues (Figs. 7 and 8) (Tari et al., 2000, 2003; 2012, 2017). This segment is also defined by a prominent downdip salt nappe and fold-thrust belt (Tari and Jabour, 2013) recording the highest magnitude (c. 14–20 km) and rate of salt and overburden translation in the entire margin (Figs. 3–7). The magnitude is estimated based on the distance from the frontal edge of the nappe to the original limit of the salt basin, which coincides with a large landward-dipping pre-salt fault (Fig. 7). Middle Jurassic-Aptian growth synclines are capped by a broadly isopachous Albian interval in the salt-cored fold-belt over the nappe suggesting translation occurred during that period and, therefore, at c. 0.2–0.4 km/Ma (Fig. 7). Although within the range of salt-flow rates described for passive margins (Rowan et al., 2004; Peel, 2014b), these values are generally lower than rates reported for post-rift salt basins (up to 0.8 km/Ma) such as Angola and Brazil (Peel, 2014b; Pichel et al., 2018a).

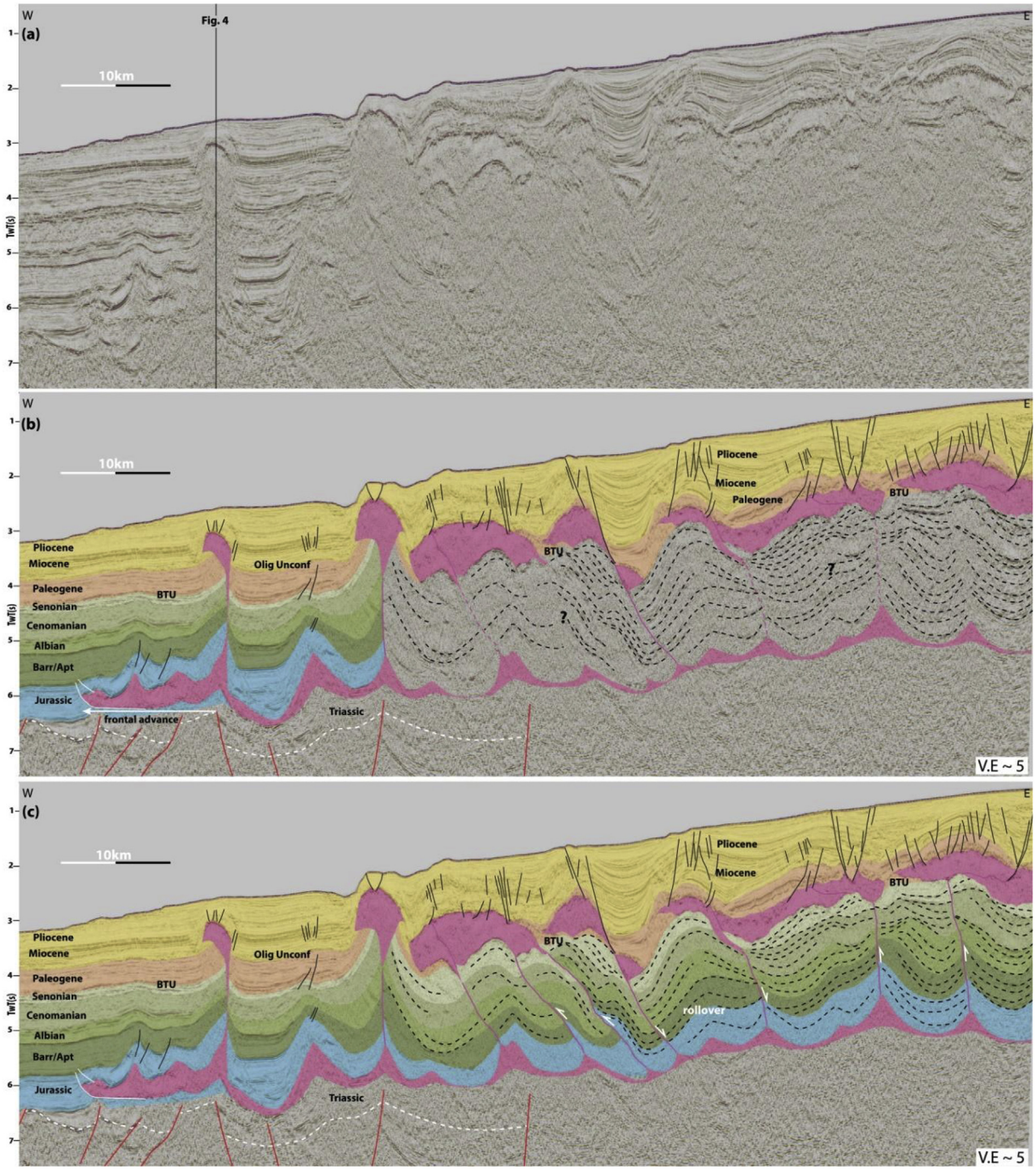

Fig. 7. (a) Uninterpreted, (b) semi-interpreted and (c) fully-interpreted regional seismic section offshore Essaouira showing the widespread occurrence of allochthonous salt sheets and canopy fed by sub-vertical to seaward-leaning feeders exhibiting complex kinematics and along-dip alternation of extensional (basinward-dipping rollovers) and contractional provinces (reverse shearing and folding). The downdip end of the basin is characterized by a c. 15 km wide salt nappe and sub-vertical squeezed diapirs with asymmetric salt tongues. Sub-salt dashed-lines are used for faults (red) and the Base-Triassic horizon (white), which are subject to uncertainties due to typical sub-salt imaging issues but can be inferred based on a combination of supra-salt geometries and sub-salt seismic facies variations and truncations. The relative displacements of minibasins are indicated by white arrows. Vertical Exxageration is c. 5-fold based on an average velocity of 4000 m/s. (For interpretation of the references to colour in this figure legend, the reader is referred to the Web version of this article.)

3D data images the largest salt canopy in the basin together with a number of other smaller allochthonous sheets (Figs. 3 and 9-13). TWT structure maps of the top and base-allochthonous salt (Fig. 9a and b) show a canopy with an area of 1390 km^2, maximum thickness of c. 2.7–2.9 km and an average thickness of 1.2 km (Fig. 9c). The identification of semi-circular lows at the base- and top-canopy levels (Fig. 9a and b) aligned with steep seaward-leaning sub-salt truncations and salt pedestals at the autochthonous level in cross-section (Figs. 8 and 10-12), permitted confident interpretation of at least five individual feeders (Fig. 9). These feeders indicate that the canopy formed by the coalescence of a minimum of five smaller salt sheets due to early downdip gliding and spreading.

The recognition of individual sheets and their associated feeders permitted interpretation of the kinematics and growth patterns in various sub-salt minibasins. The allochthonous salt sheets are linked to the autochthonous level by predominantly counter-regional (*sensu*

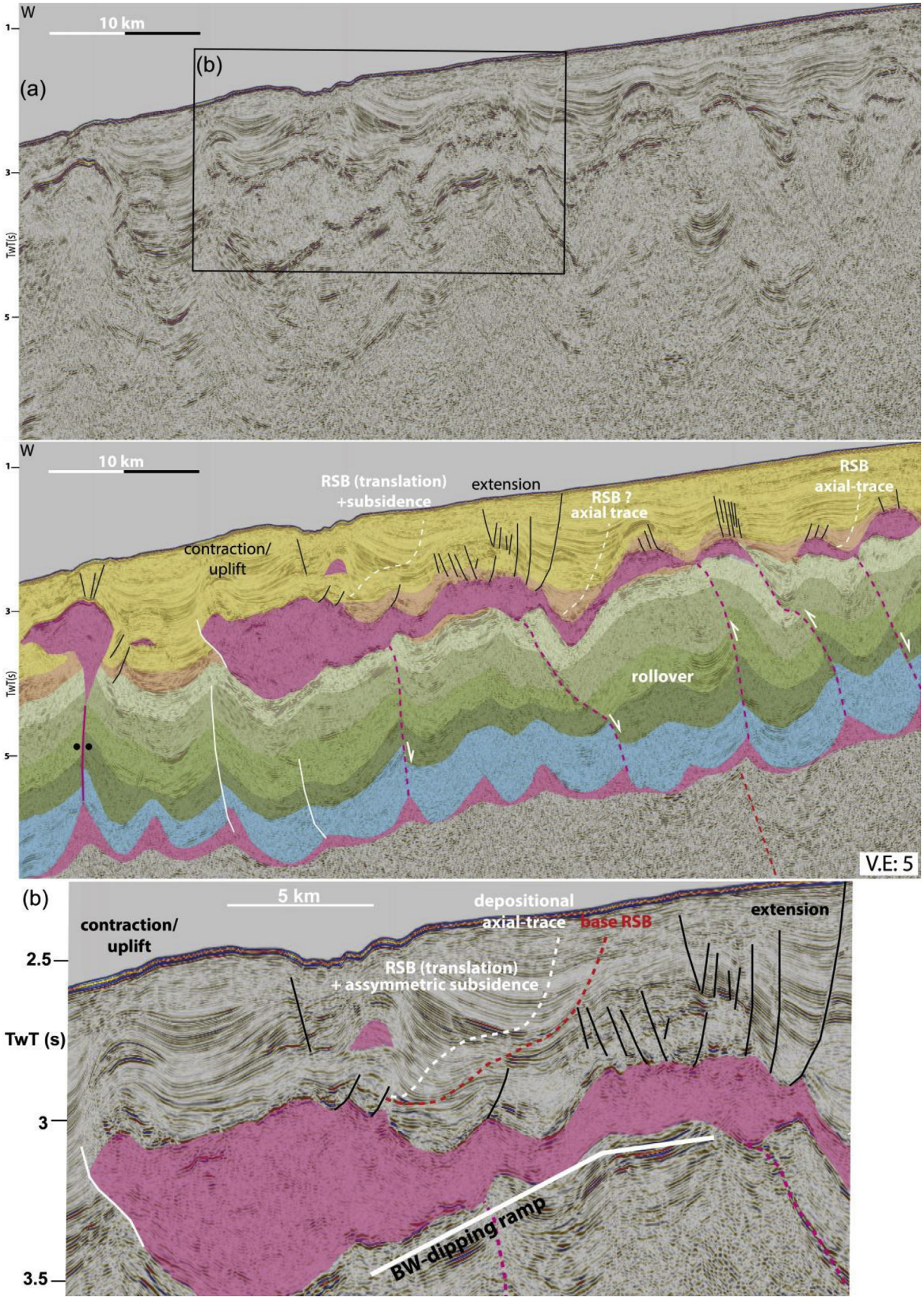

Fig. 8. (a) Uninterpreted and interpreted regional seismic section offshore Essaouira showing the widespread occurrence of allochthonous salt sheets and a c. 35 km wide canopy fed by sub-vertical to seaward-leaning feeders exhibiting complex kinematics and along-dip alternation of structural styles. Allochthonous salt sheets exhibit updip extension, intermediate landward-thickening asymmetric minibasins (i.e. RSBs) formed over basinward-dipping base-salt ramps and recording 8 km of translation; passing downdip to zones of uplift and contraction. Zoom in (b). Vertical Exxageration is c. 5-fold based on an average velocity of 4000 m/s.

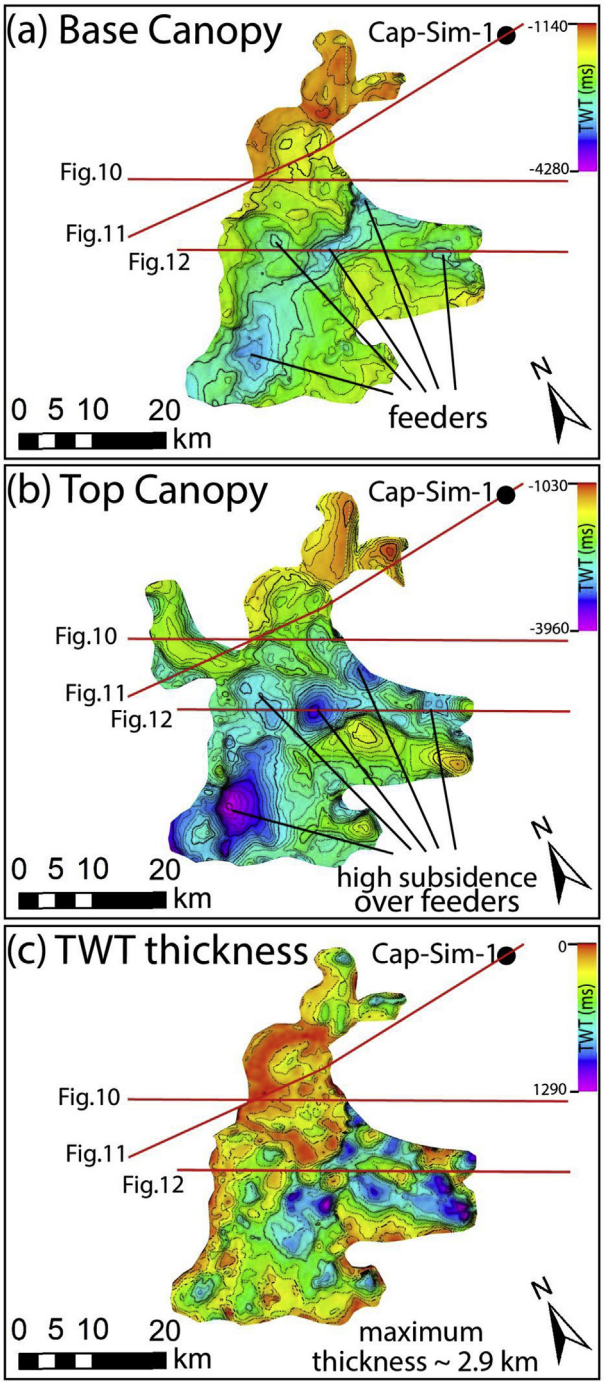

Fig. 9. (a) base, (b) top and (c) thickness map of the allochthonous salt canopy in Essaouira generated from the 3D seismic dataset with the approximate location of 3D seismic sections presented in Figs. 10–12. The location of feeders and original smaller sheets are identified by base-salt and top-salt lows and ramps.

Schuster, 1995), seaward-verging and apparently-welded feeders associated with variable geometries and growth strata (Figs. 7–13). They can be associated with expulsion and/or extensional rollovers (c.f. Ge et al., 1997; Krézsek et al., 2007; Jackson et al., 2015a) where hangingwall strata dip gently basinward and thicken towards the feeders, subsiding relative to its footwall further downdip (Figs. 7 and 8). Their hangingwalls can also dip dominantly landward and sub-parallel to the feeders showing a reverse sense of movement relative to the footwall, thinning towards the feeders and fold-geometries suggestive of thrust-related folding (c.f. Shaw et al., 2005; McClay et al., 2011) and contraction (Figs. 7, 8, 10,12 and 13).

These variations indicate an early evolution and emplacement of allochthonous salt linked to at least two different mechanisms: i) extension and/or subsidence of supra-salt strata leading to seaward salt expulsion, and ii) contraction and uplift. These mechanisms alternate downdip and along-strike with zones of uplift and contraction passing downdip to areas of extension and salt expulsion, and further downdip to another zone of contraction (Figs. 7-8a-b, 10 and 12–13). This structural zonation challenges the conventional view of regional gravity-driven salt deformation in passive margins where updip extensional domains are linked to downdip basin edge contractional provinces by a broadly undeformed translational zone (c.f. Rowan et al., 2004; Brun and Fort, 2011; Quirk et al., 2012; Jackson et al., 2015a).

3D seismic data provides a more detailed picture of these complex minibasin geometries, showing that hangingwall strata associated with counter-regional feeders commonly present switches in their kinematics and growth pattern through time (Figs. 10–13). The landward minibasin (A, Fig. 10) and its seaward-verging salt feeder show an early history of subsidence and basinward-thickening associated with a Jurassic rollover, followed by stratal thinning and uplift against the same feeder in the Early Cretaceous-Cenomanian indicating lateral contraction and thrusting. The minibasin immediately downdip (B, Fig. 10) presents the opposite growth history. Thinning, buckling and thrust-related folding of the Middle Jurassic interval indicates Jurassic contraction and thrust salt-piercement; passing upwards within the same minibasin to Early Cretaceous-Cenomanian basinward subsidence and thickening (Fig. 10). The associated feeders change from gently-dipping in response to the vertical load associated with minibasin subsidence and basinward-thickening strata, to sub-vertical due to lateral displacement loading related to shortening and diapir squeezing (Figs. 10 and 11).

General thinning and uplift of Senonian-Paleogene strata towards squeezed salt stems indicate a regional pulse of contraction and inversion (Figs. 10–13). This coincides with periods of regional thick-skinned contraction both onshore and offshore Morocco (Hafid et al., 2006; Tari and Jabour, 2013), suggesting late minibasin inversion was driven by basement-involved contraction and uplift. A large, 10–15 km wide present-day bathymetric high, cored by a zone of uplifted and possibly inverted basement and with a squeezed diapir at its centre suggests basement-involved inversion is still ongoing and greater northeastwards in the Essaouira Basin (Fig. 11). Despite poor imaging of the pre-salt interval, the presence of shallower autochthonous salt at this portion of Essaouira and uplift of a > 1 km thick roof by the squeezed diapir support an interpretation of basement-involved contraction and inversion of syn-rift faults (Fig. 11), as diapirs are typically not capable of uplifting such a thick roof purely by buoyancy (Jackson and Hudec, 2017).

At the allochthonous level, salt deformation is characterized by the alternation of kinematically-linked domains of extension, translation and contraction, indicating basinward movement of salt and overburden and the influence of base-salt relief (Figs. 7, 8 and 10–13). Updip extension is represented by listric basinward-dipping normal faults and extensional, landward-thickening rollovers (Figs. 5, 7 and 8). These occasionally define roho-systems (*sensu* Schuster, 1995; Rowan et al., 1999) (updip sheets in Figs. 7 and 11) and may be associated with small salt rollers and nearly-welded salt due to large basinward salt evacuation (Fig. 11). Contraction is characterized by folding and uplift of roof strata with outer-arc extension (keystone faults) or squeezing and steepening of their landward-dipping frontal edge (Figs. 7 and 8). The amount of extension is generally greater than the observed contraction, suggesting extension and downdip gliding were initially accommodated by open-toe salt advance (*sensu* Hudec and Jackson, 2006) as the sheets were emplaced at or near the sea-floor. In wider (> 5 km) sheets and canopies, extension is usually linked to downdip contraction

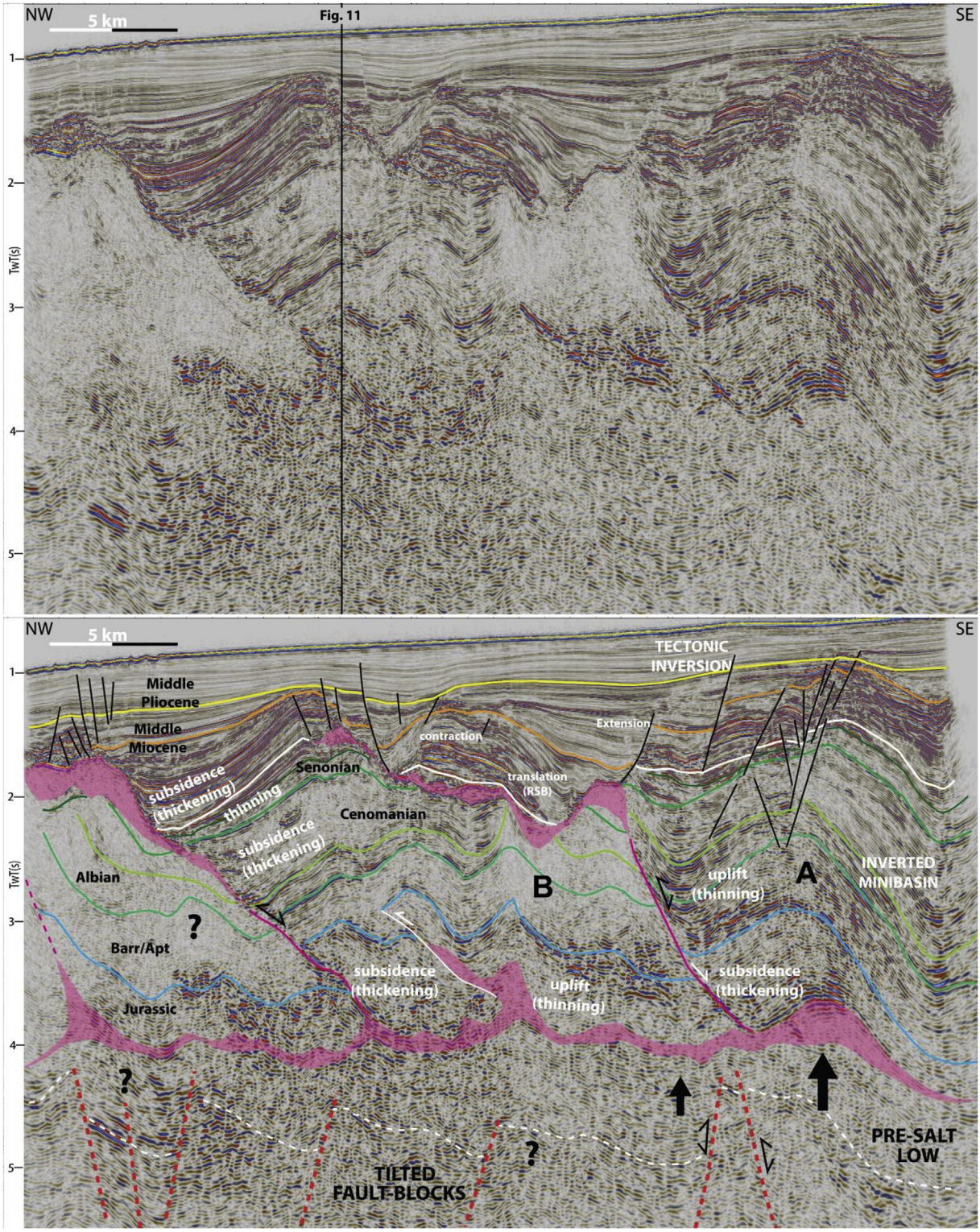

Fig. 10. Uninterpreted and interpreted 3D seismic section showing complex kinematics on over both autochthonous and allochthonous salt. Updip minibasin shows Jurassic basinward-thickening rollover passing upward to thinning Lower Cretaceous section against a seaward-leaning squeezed feeder that originates a c. 10 km wide salt sheet. The minibasin further downdip shows the opposite growth history with Jurassic buckle-folding and thrusting indicating contraction passing upward to basinward-dipping and thickening Cretaceous section. Both minibasins are then inverted and contractionally deformed during the Senonian to Paleogene. These geometries can guide the estimation of pre-salt structures below (dashed lines). The allochthonous sheet is defined updip by basinward-dipping normal faults, intermediate translation (RSB) and uplift passing to a zone of counter-regional flow at its landward-dipping downdip edge. Black arrows denote uplift related to thick-skinned tectonics and reactivation of pre-salt rift faults, with their size quantitatively denoting the magnitude of uplift.

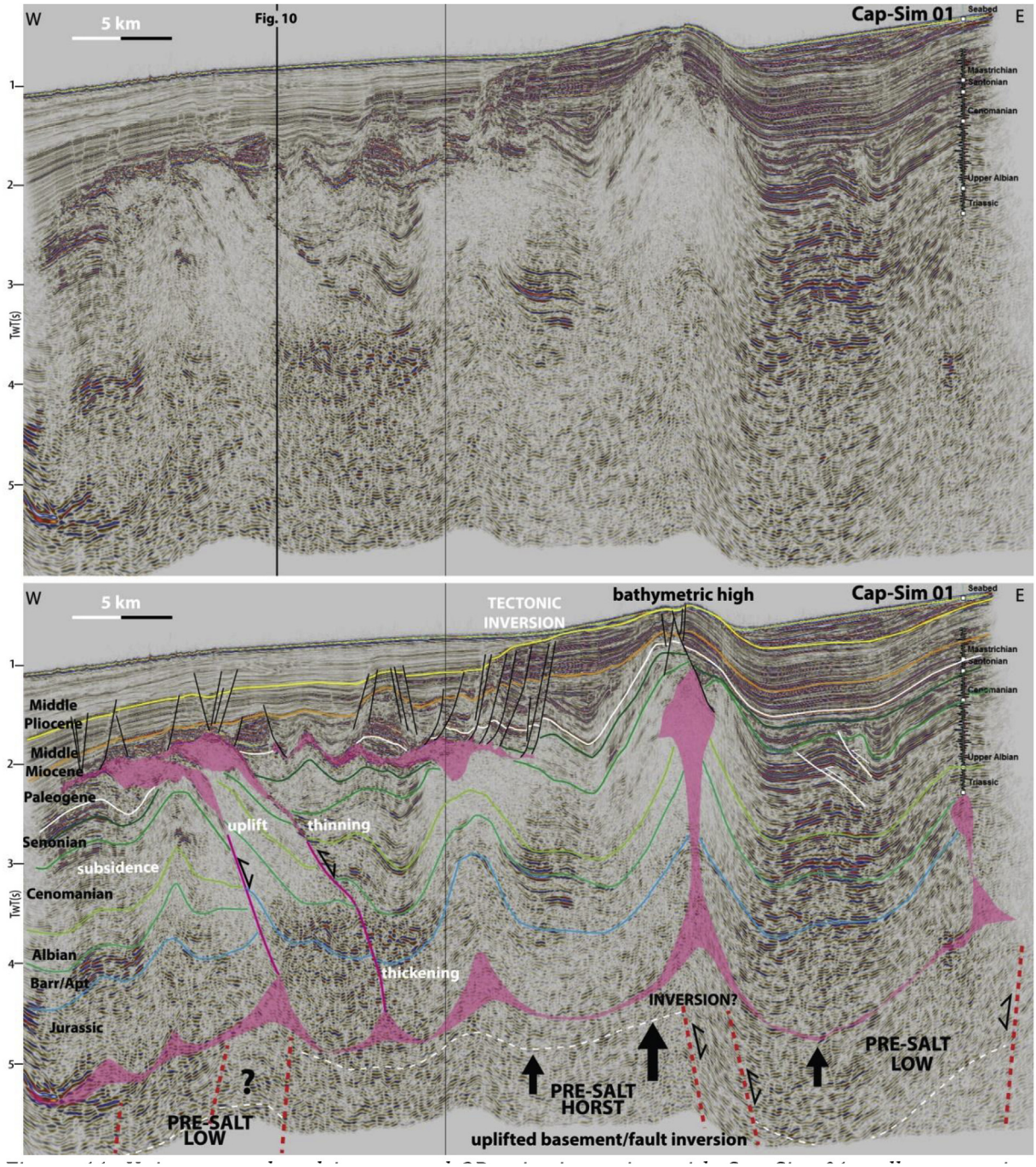

Fig. 11. Uninterpreted and interpreted 3D seismic section with Cap-Sim 01 well penetrating Upper Albian and Triassic salt without Aptian and Jurassic section indicating the presence of a diapir. The section illustrates a highly squeezed sub-vertical diapir uplifting a c. 1 km thick roof and generating sea-floor topography. The smaller volume of salt and shallower autochthonous salt allow identification of certain pre-salt rift geometries (dashed lines) that indicate uplift and inversion of syn-rift faults. Further downdip a thin Senonian allochthonous sheet with salt rollers and basinward-dipping normal faults indicates downdip gliding and salt evacuation. Further basinward, two stacked salt sheets nucleate from seaward-leaning feeders over the top-Cretaceous interval. Feeders show complex kinematics and multiphase growth patterns with early basinward-thickening and later basinward-thinning indicating inversion.

by an intermediate zone of translation where landward-dipping growth strata define Ramp-Syncline Basins (RSBs, c.f. Pichel et al., 2018a). These basins were initially described to form above autochthonous salt by translation over basinward-dipping base-salt ramps (Jackson and Hudec, 2005), and here they develop by movement over similar ramps but at an allochthonous level (Figs. 7, 8, 10, 12 and 13).

These minibasins are strongly asymmetric, being characterized by predominantly landward-thickening sigmoidal strata and a basinward-dipping axial trace (Figs. 7, 8, 12 and 13). They may directly onlap the top of the salt sheet indicating translation started immediately after extrusion (Figs. 10–13); or a thin (c. 100–200 m thick) pre-kinematic cover where the initial translation occurred over a flat surface or, alternatively, started later (Figs. 7 and 8). They terminate updip above a base-salt basinward-dipping ramp, being occasionally near but not in direct contact with basinward-dipping normal faults (Figs. 7, 8 and 10); and in places appear highly rotated and onlapping a steep landward-dipping top-allochthonous salt (Figs. 12 and 13). These relationships indicate they are not directly driven by basinward-dipping normal

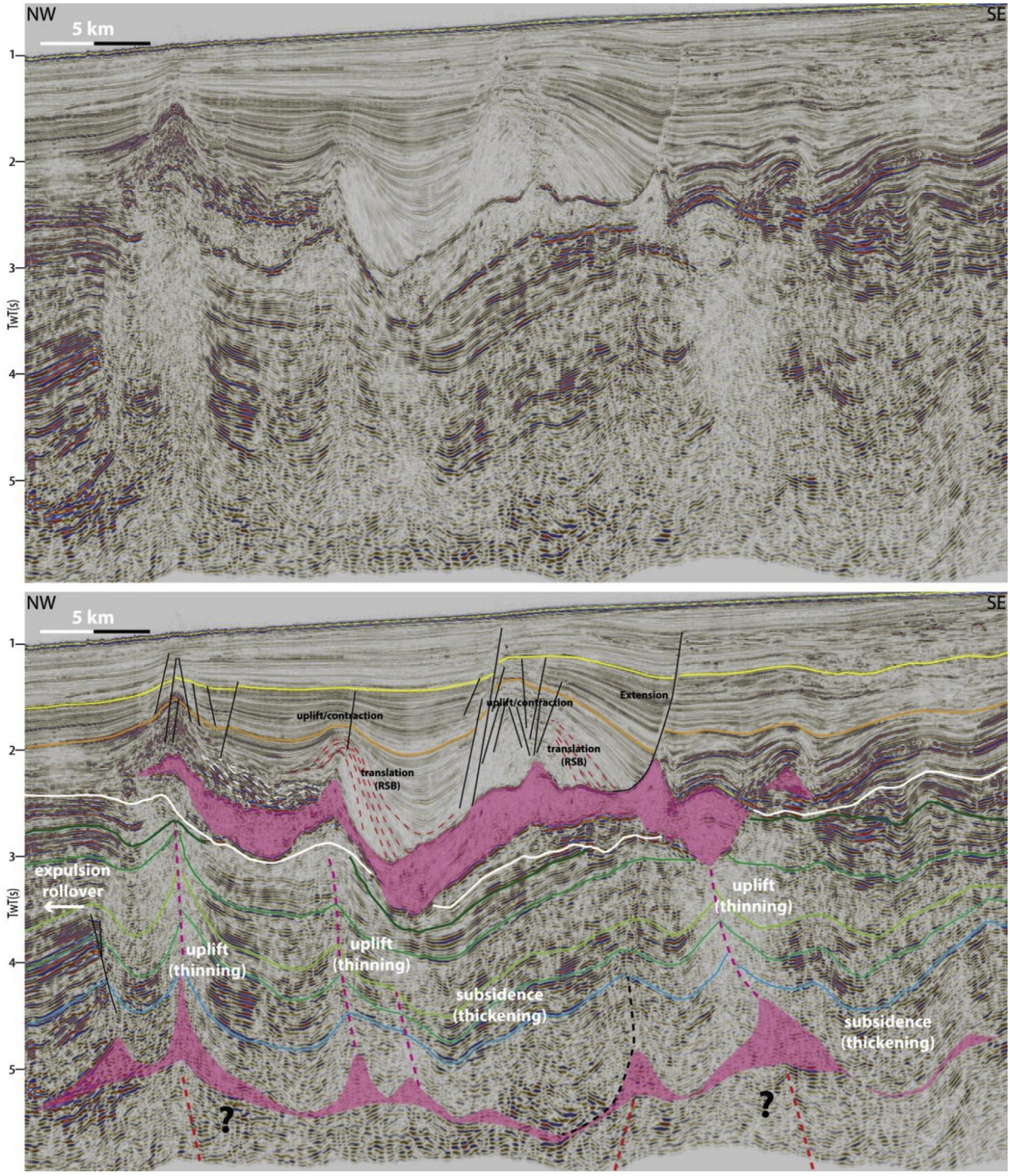

Fig. 12. Uninterpreted and interpreted 3D seismic section showing complex kinematics on top of the allochthonous salt canopy in the Essaouira Basin, with pairs of updip extension, translation defined by ramp-syncline basins (RSB) and downdip uplift and contraction. Mesozoic sub-salt strata also show similar alternation and multiphase evolution of minibasins and salt feeders that originate the allochthonous salt sheets, with zones of basinward-thickening passing downdip to zones of uplift and basinward-thinning. Pre-salt rift structures (red dashed lines) are estimated based on supra-salt architectures and wedge geometries and truncation patterns below autochthonous salt. (For interpretation of the references to colour in this figure legend, the reader is referred to the Web version of this article.)

faults, but form by salt and overburden translation in response to extension further updip (Figs. 7, 8, 12 and 13). Their asymmetry and landward-vergence also discredit the hypothesis that they are driven purely by salt expulsion, because in that case, they would be symmetric and with vertically-aligned axial-traces (i.e. bowls *sensu* Rowan and Weimer, 1998). Expulsion, nevertheless, played a second-order control on their kinematics, because as RSBs thicken, they imposeincreasing load onto the underlying salt and, as the salt thins, they tend to translate progressively slower (Jackson and Hudec, 2005; Pichel et al., 2018a). This increased the relative importance of load-driven subsidence and salt expulsion over time until the salt was drastically thinned, resulting in progressively more symmetry in the upper section of the RSB (Figs. 7, 8, 12 and 13).

A total of 9–10 km basinward translation is estimated by measuring the distance of the first, basinwardmost onlap point and/or depositional axial-trace to the top of the base-salt ramp (Figs. 7–8) (c.f. Jackson and Hudec, 2005). This amount of translation, however, only accounts for the period when the salt canopy was already formed because individual

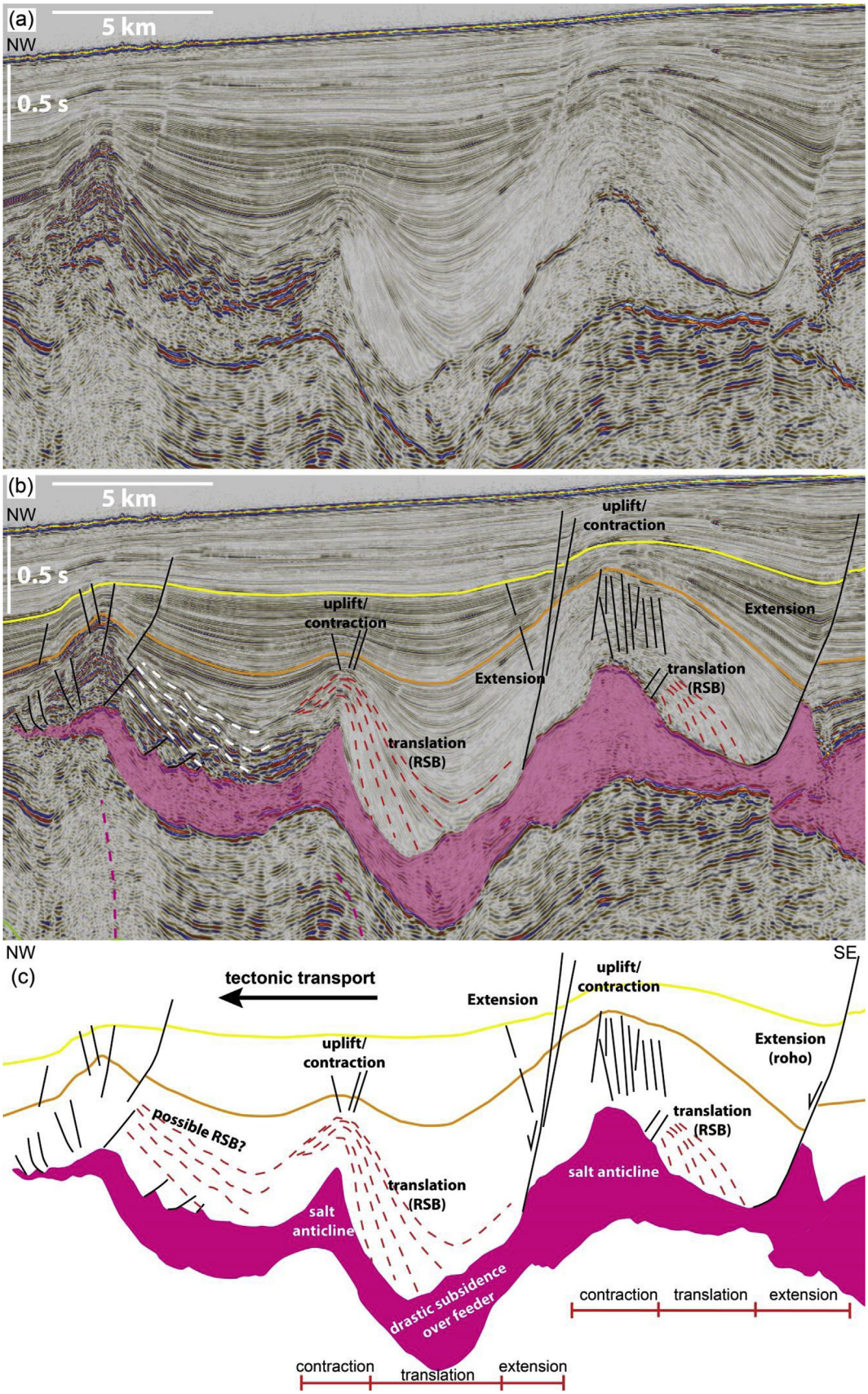

Fig. 13. (a) Uninterpreted and (b) interpreted 3D seismic section zooming on ramp-syncline basins (RSB) systems formed above the largest allochthonous salt canopy offshore Morocco. (c) Schematic diagram illustrating the complex kinematics associated with gliding on top of allochthonous salt sheets with drastic initial thickness variations and very irregular base-salt topography, which results in the development of alternate domains of updip extension, translation (RSB) and downdip contraction. Translation and salt expulsion work in tandem generating accommodation, with expulsion becoming gradually stronger where salt was initially thicker (e.g. feeders).

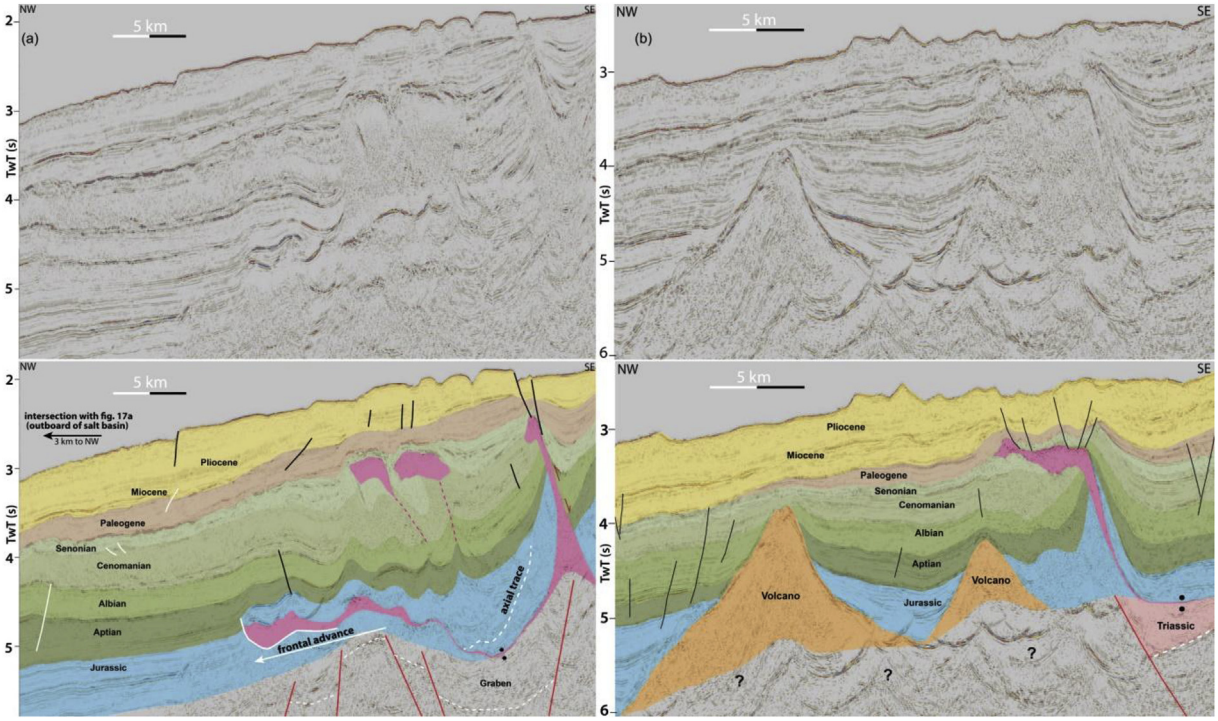

Fig. 14. Uninterpreted and interpreted sections of (a) southern portion of Safi segment showing 8 km wide salt nappe and salt-cored folds indicating frontal advance from the downdip edge of the salt basin over a c. 10 km wide pre-salt graben. A thick Jurassic-Cretaceous minibasin forms by increased subsidence near the graben basinward-dipping fault; passing downdip to a sub-vertical squeezed feeder with multiphase growth and small salt tongue at its crest. In (b) large volcanoes defined the downdip edge along the centre of the Safi segment, acting as strong buffers to downdip salt flow (Tari and Jabour, 2013), favouring contraction and upward movement of salt resulting in the development of a steep seaward-leaning feeder by reverse shearing and allochthonous sheet. Vertical Exxageration is c. 5-fold based on an average velocity of 4000 m/s.

sheets would not have merged after being deeply buried by sediments. They are likely to have coalesced early (c.f. Dooley et al., 2012), immediately after their extrusion over a depositional hiatus prior to, or early in, the history of the RSBs, indicating that additional, early salt translation occurred without having a record in the overburden that allows its quantification. The contractional and extensional domains associated with these RSBs (Figs. 10 and 12) are, therefore, formed after or late during the coalescence of individual salt sheets, indicating their development is controlled by the relief at the base of the canopy (c.f. Dooley et al., 2018).

4.2.3. Safi Basin

The northernmost segment, termed the Safi Basin, corresponds to a considerably narrower (40–45 km wide) and steeper (c. 5° of base-salt dip on average) salt basin, with reduced salt volume and a resultant smaller number of structures than segments further south (Figs. 3 and 14-16). This segment is also characterized by the thinnest overburden in the study-area, being on average only 3.5–4 km thick (Figs. 14–16).

To the southwest, near the Essaouira segment, a c. 10 km wide salt nappe has advanced c. 10 km basinward from the downdip edge of the salt basin defined by a relatively symmetric 10 km wide pre-salt graben (Fig. 14a). This salt nappe comprises a frontal thrust and salt-cored fold belt linked updip to a c. 3.5 km thick, welded Jurassic-Upper Cretaceous minibasin. The minibasin contains an asymmetric, landward-thickening Jurassic growth section defined by a basinward-dipping axial-trace characteristic of ramp-syncline basins (RSBs, Pichel et al.,

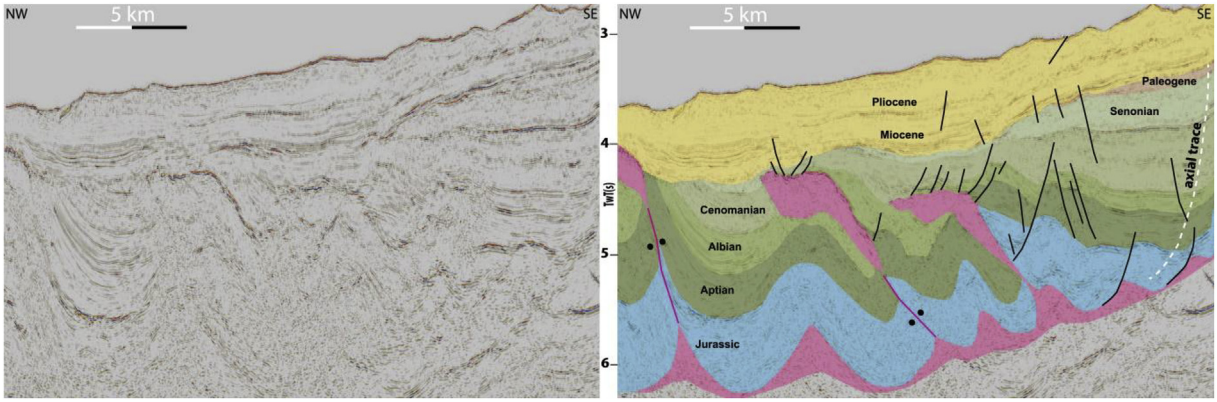

Fig. 15. Uninterpreted and interpreted sections of the Safi segment showing early (Albian-Cenomanian) development of allochthonous salt tongues associated with counter-regional, seaward-leaning feeders formed by contraction and thrusting of the hangingwall over the feeders. Minor updip extension (small salt rollers and basinward-dipping normal faults) occurs during the Jurassic, passing upwards to an asymmetric, landward-dipping growth section, possibly associated with a ramp-syncline basin.

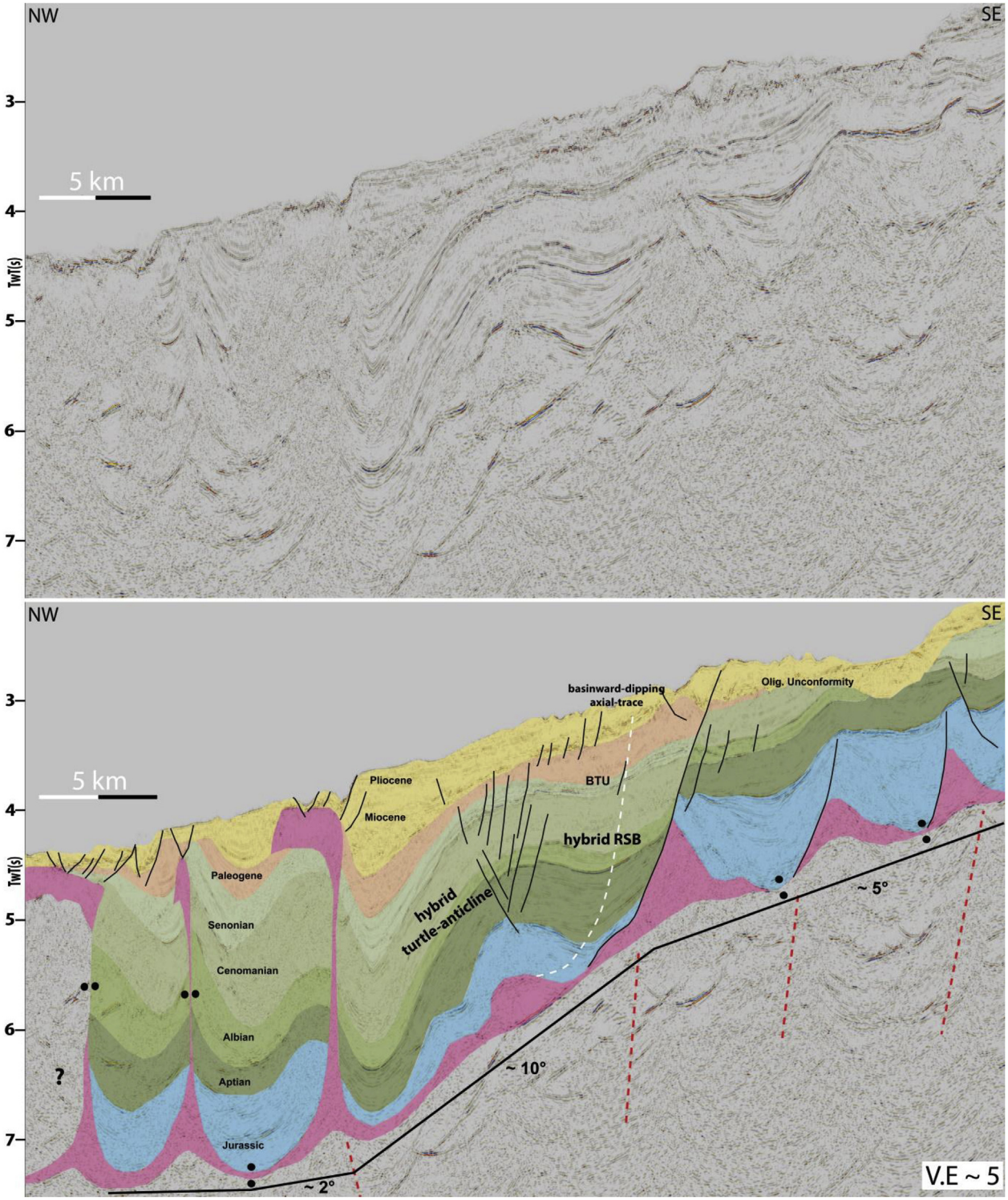

Fig. 16. Uninterpreted and interpreted sections of the northern end of Safi Basin (Tari and Jabour, 2013) showing a narrow kinematically-linked system of updip extension with basinward-dipping normal faults and roller; intermediate translation with a hybrid RSB and turtle anticline over a steep basinward-dipping base-salt ramp; passing downdip to highly-squeezed sub-vertical diapirs and salt tongues. Vertical Exxageration is c. 5-fold based on an average velocity of 4000 m/s.

2018a). This suggests it formed by a combination of load-driven subsidence and translation over thick salt at the updip edge of the graben, promoting basinward salt expulsion towards the nappe (Fig. 14a). Over its updip footwall, a basinward-verging nearly-welded salt wall with a c. 1 km wide tongue at its crest is associated with Jurassic-Early Albian growth strata showing evidence of subsidence towards the wall; whereas Late Albian-Paleogene strata are upturned and uplifted, suggesting later inversion (Fig. 14a). Cenozoic salt movement is less pronounced in this segment, as salt structures become buried by a Late Cretaceous-Paleogene section, possibly due to the smaller salt supply in the area (Fig. 14). Nevertheless, ongoing activity is recorded by a few structures, as seen by normal faulting at the crest of the basinward-leaning and rising diapir at the updip edge of the graben (Fig. 14a).

Large (3–4 km high and at least 10 km wide) flat-based conical

features interpreted as volcanoes (Dunlap et al., 2010; Tari and Jabour, 2013) occur in the central portion of this segment (Fig. 14b). The base of the volcanoes occurs at the same stratigraphic level as the base of autochthonous salt suggesting both originated at/near the same time at the end of rifting during the Late Triassic-Early Jurassic (Fig. 14b). These tall volcanoes generated additional topography during salt deposition with salt being deposited around but not on top of them. They acted as topographic barriers, limiting early (Jurassic-Lower Cretaceous) downdip gliding and salt advance, and thus, inhibiting the development of a salt nappe in this part of the basin (Figs. 3 and 14b) (Tari and Jabour, 2013). Additionally, they promoted increased and early downdip contraction and upward salt flow on their landward side (c.f. Ferrer et al., 2017), as shown by uplift and reverse shearing/thrusting of the updip minibasins against seaward-leaning squeezed diapirs during the Jurassic-Early Cretaceous (Figs. 14b and 15). This also resulted in earlier development of small (3–5 km wide) salt sheets during the Albian-Cenomanian due to diapir squeezing (Figs. 14b and 15).

Further northwards, near the limit of this segment, the margin becomes steeper and a large (30–35 km) linked gravity-driven system is developed (Fig. 16). This system is characterized by updip Jurassic-Aptian rafts and associated 2–4 km amplitude salt rollers and basinward-dipping listric faults. This domain transitions downdip to a 5–10 km wide translational province formed over a considerably steeper (c. 10°) salt detachment associated with a large base-salt ramp (Fig. 16). In this translational domain, a hybrid turtle anticline formed by a combination of salt expulsion and updip extension over a large (3.5 km tall), basinward-dipping normal fault with a ramp-flat geometry (*sensu* McClay, 1990, 1996). This fault is defined basinward by a Jurassic extensional-rollover, passing upwards to an extension-driven and salt-influenced RSB (c.f. McClay, 1990, 1996; Roma et al., 2018a); recording c. 7 km of salt and overburden downdip translation (Fig. 16). The hybrid turtle anticline overlies an inflated salt (c. 1 km thick anticline) at its centre (Fig. 16), having a different geometry to classical turtle anticlines (*sensu* Vendeville and Jackson, 1992) in which the underlying salt is nearly or completely exhausted (c.f. Jackson and Hudec, 2017). This implies that subsidence and salt expulsion are not focused at the centre of the minibasin and that these hybrid examples are primarily driven by extension and translation. Subsidence is focused over the normal fault, so while sediments accumulate there, previous strata translate and rotate basinward resulting in a landward-thickening succession (hybrid RSB) and downdip salt inflation (Fig. 16). At the downdip end of this turtle, a thinned Jurassic-Aptian section overlying nearly welded salt passes upward to thickened Cenomanian-Paleogene strata, both of which synformally folded and associated with a vertical squeezed feeder (Fig. 16). In the downdip domain, highly squeezed subvertical salt walls associated with buckle-fold geometries within their minibasins and 2–5 km wide allochthonous salt sheets indicate deformation was mainly driven by contraction (Fig. 16). As evidenced by extension and translation further updip, contraction occurred as the system moved over a base-salt contractional hinge at the downdip end of the basin where the base-salt flattens and flow decelerates abruptly (Fig. 16) (c.f. Dooley et al., 2016, 2018).

5. Impact of thick-skinned tectonics

The effects of thick-skinned contraction related to the Alpine/Atlas Orogeny have been described by a number of authors, both onshore and offshore along the margin (Hafid et al., 2000, 2006; Tari et al., 2012, 2017; Tari and Jabour, 2013; Vergés et al., 2017). Although recognized to have an impact on salt tectonics and basin morphology, these previous studies did not investigate how these broadly N-S-oriented contractional events affected the kinematics and style of salt deformation offshore.

A series of NW-SE-trending basement-involved folds had been recognized outboard of the salt basin along the Safi segment by Tari et al. (2012), formed by reactivation and inversion of syn-rift normal faults (Fig. 17a) (Tari and Jabour, 2013). As these folds are located basinward of the salt basin, thickness variations and growth strata can be used as confident indicators of the timing and kinematics of these salt-unrelated events. A broadly isopachous Jurassic-Cenomanian succession is folded over 10–15 km wavelength basement-involved folds, cored by inverted syn-rift faults and uplifted basement (Fig. 17a). The folds present rounded to box-fold geometries, being offset by predominantly NE-verging reverse faults (Fig. 17a). Senonian-Paleogene growth strata onlap and thin towards the crest of this structure, being capped by a broadly isopachous folded Neogene succession with greater thickness variations occurring in the Paleogene interval (Fig. 17a). These stratal patterns indicate that thick-skinned contraction started during the Senonian, became stronger during Paleogene-Miocene and reduced during the Pliocene-recent, although it is still ongoing as demonstrated by the folded present-day seafloor (Fig. 17a).

Further south, near the large salt nappe in Essaouira, there is evidence of both salt-related and thick-skinned N-S contraction (Fig. 4). North of the salt nappe, the thick, broadly tabular Jurassic-Cenomanian interval is folded and onlapped by Senonian-Paleogene growth strata and truncated by the BTU and Paleogene unconformities (Fig. 4). Over the southern edge of the nappe, a triangular salt roller is associated with a northward-dipping listric normal fault with Jurassic asymmetric growth strata at its hangingwall (Fig. 4). Lower Cretaceous growth is dramatically reduced, as seen by a nearly isopachous, albeit folded, section that is uplifted above regional over the fault and onlapped by Senonian-Paleogene strata, indicating that the fault and earlier extensional rollover were inverted during this time (Fig. 4).

At the updip end of the basin between Agadir and Essaouira (Fig. 3), a NW-SE-oriented profile images another example of roughly W-E salt-related contractional structures (Fig. 17b). A N-NW verging salt-cored box-fold and a tear-drop diapir developed in the shelf involving a broadly isopachous Late-Jurassic-Early-Cretaceous interval that is onlapped by late Cenomanian-Paleogene growth strata and truncated by equivalent unconformities (Fig. 17b). Earlier, Middle-Jurassic growth occurred but this was minor as indicated by a broadly tabular Aptian-Cenomanian interval that was later upturned and broken apart by the squeezed diapir (Fig. 17a). Although there is no clear evidence of basement-involved reactivation due to sub-salt resolution issues (Fig. 17b), the E-W orientation of these highly squeezed salt structures, the location at the shelf, and timing of movement indicate they are also associated with the same Late Cretaceous-Cenozoic contractional event (Fig. 17). Due to their position and orientation, we may also speculate that they correspond to the continuation of a salt-cored fold at the edge of the continent (Cap-Ghir Anticline, Luber, 2017).

These lines of evidence can be extended towards the more complex, central areas of the basin, where pronounced salt tectonics partially obscures signals of basement-involved contraction. The widespread occurrence of shortening-driven minibasins and squeezed diapirs, many of which currently active and uplifting thick roofs (up to c. 1.5 km) over the shelf and entire slope in Agadir-Essaouira (Fig. 5), suggest an important contribution from late thick-skinned contraction. 3D seismic data, which offer better illumination of sub-salt intervals, shows proximal areas where the autochthonous salt and entire overburden are uplifted c. 1–2 km above regional at the north-northeast of Essaouira (Figs. 10 and 11).

Although the data does not afford clear visualization of basement structures throughout, where the allochthonous salt is thinner, it is possible to observe pre-salt geometries (i.e. tightening and uplift of syn-rift hangingwall folds, Figs. 10–11) that indicate contraction and inversion of syn-rift structures. This area coincides with the location of the Tafelney Accommodation Zone (TAZ, Tari and Molnar, 2005; Tari et al., 2012), an oblique NW-SE syn-rift high that could have acted as a favourably-oriented weakness zone preferentially accommodating most of the N-S to NE-SW contraction in the basin. This resulted in an additional contraction of salt feeders and diapirs, and further tilting that

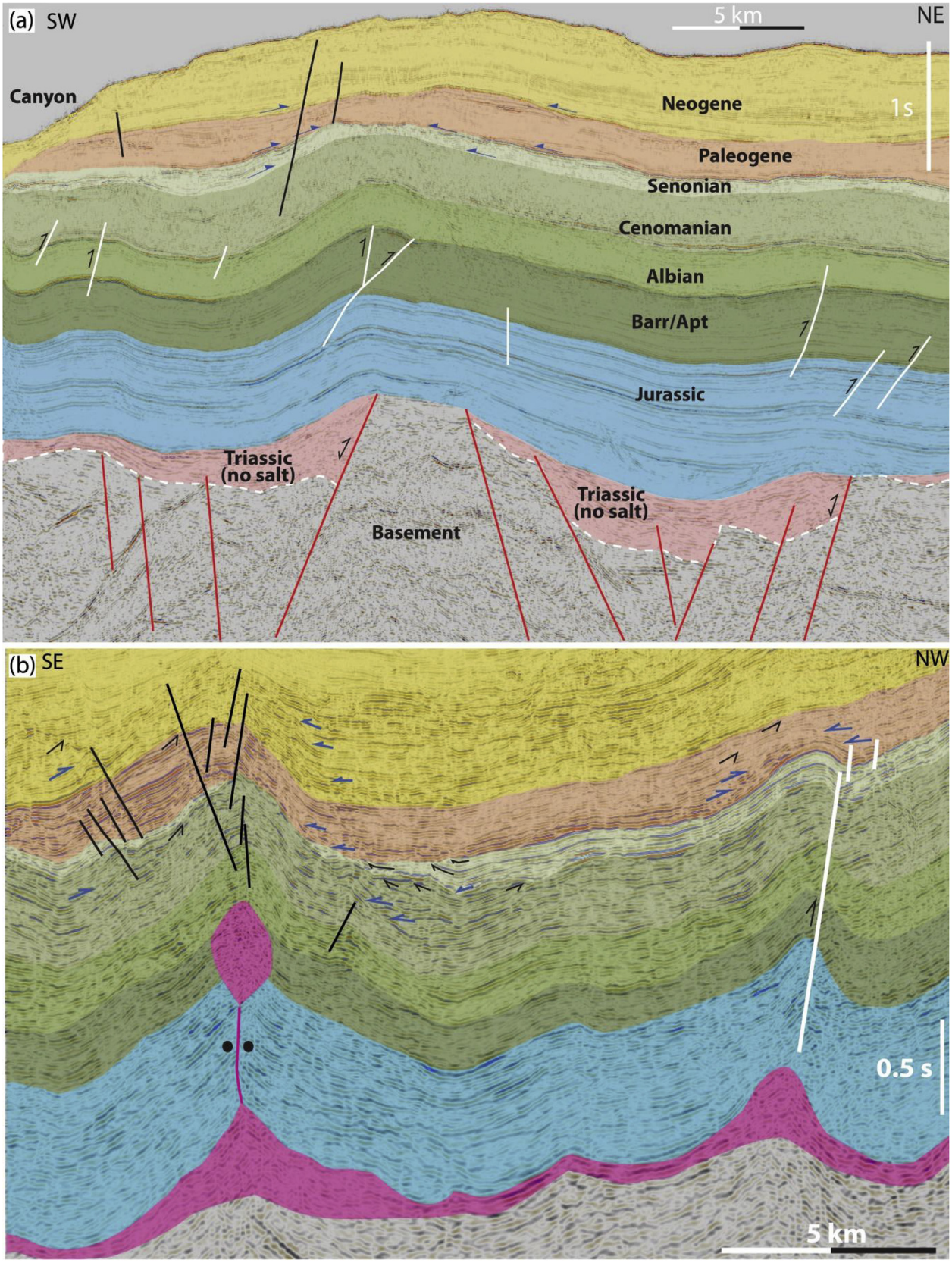

Fig. 17. (a) Strike-oriented section outboard of the salt basin in Safi, showing inversion of pre-salt normal faults, basement-involved folding and reverse faulting of a broadly isopachous Jurassic-Cenomanian succession onlapped by Senonian-Neogene strata. (b) Strike-oriented section at the shelf-edge in Agadir Basin showing two pulses of broadly N-S contraction in the Late Cretaceous and Miocene-Pliocene. Normal faults in black and reverse faults in white lines. Erosional truncation indicated black arrows and onlaps by blue arrow denoting the main period of tectonic activity. (For interpretation of the references to colour in this figure legend, the reader is referred to the Web version of this article.)

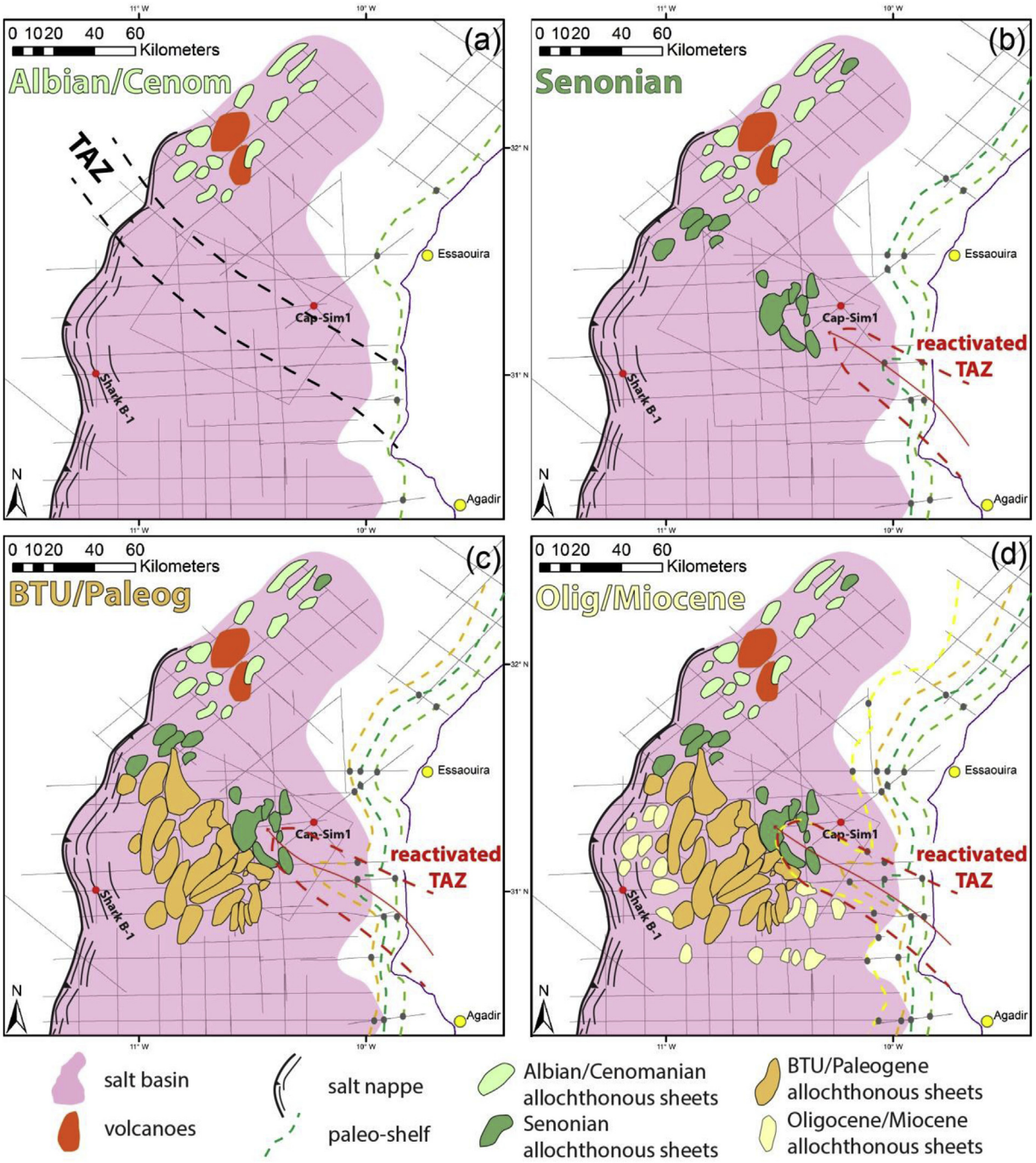

Fig. 18. Maps showing the sequential evolution of allochthonous salt sheets along the Moroccan margin during four main phases: (a) Albian-Cenomanian, (b) Senonian, (c) BTU-Paleogene, and (d) Oligo-Miocene.

enhanced basinward gliding at the allochthonous level in this portion of the basin (Figs. 7, 8 and 10-13). Moreover, it could have favoured an outward, NW-oriented salt flow, sub-parallel to the NW-plunging axis of the uplifted Tafelney Accommodation zone, and may explain the NE-SW orientation of salt sheets oblique to the margin (Figs. 1, 3 and 18).

6. Timing and mechanisms of allochthonous salt sheets generation

Multiple allochthonous salt sheets with variable geometries, dimensions, orientation and evolution occur over the Essaouira-Safi segments (Figs. 7–13 and 18). Features observed include sub-vertical to seaward-leaning diapirs with small (2–5 km wide) salt tongues, as well as large allochthonous salt sheets and canopies up to 35 km wide, 45 km long and 2.9 km thick (Figs. 7, 8 and 18). Extrusion and/or emplacement of allochthonous salt occurred during variable periods along the margin, with four major phases recognised from Albian-Cenomanian to Oligoce-Miocene (Fig. 18a–d) generally related to major erosional unconformities and/or depositional hiatuses (Figs. 7–13).

6.1. Albian-Cenomanian

The first allochthonous sheets formed during the Late Albian-Cenomanian in the northernmost Safi segment. These are characterized by NE-oriented, 3–5 km wide salt tongues that can reach up to 10 km of length (Fig. 18a). These bodies are usually associated with steeply-

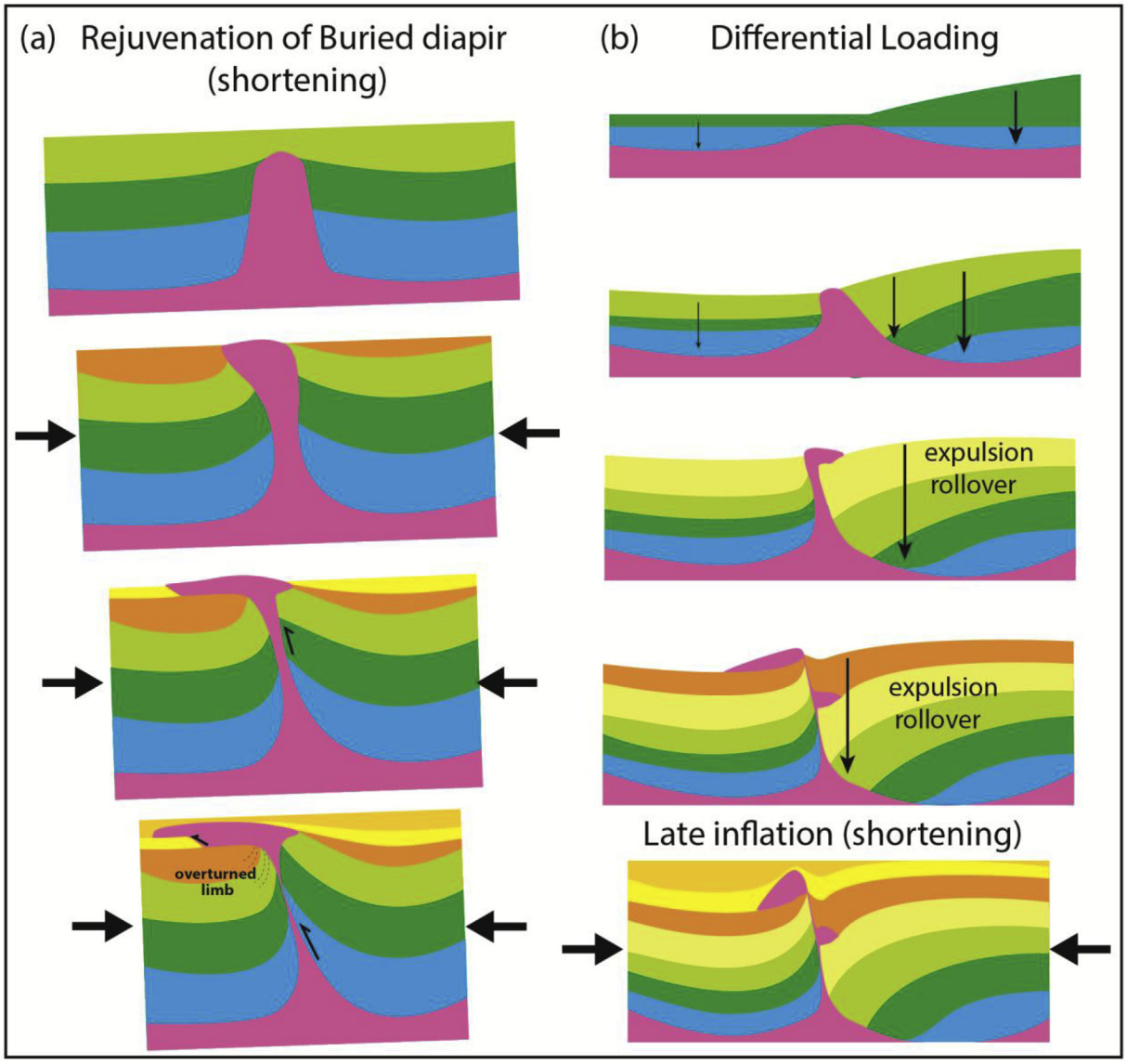

Fig. 19. Simplified, area-balanced kinematic models of end-member mechanisms leading to the development of allochthonous salt sheets in the Essaouira-Safi Basins: (a) rejuvenation of buried sub-vertical diapirs and (b) basinward expulsion rollover.

dipping landward growth strata uplifted and thrusted over footwall growth strata (Figs. 14b–15). These geometries indicate they formed by contraction at the downdip end of the basin and over base-salt contractional hinges (*sensu* Dooley et al., 2016) or against the large volcanic/basement buttresses.

6.2. Senonian

The second generation of allochthonous salt occurred during the Senonian, with the development of c. 5 km wide allochthonous sheets in the south of Safi and northeast of the Essaouira (Figs. 7 and 8), with only one small salt tongue developing further north at the edge of the Safi Basin (Figs. 15 and 18b). The first allochthons appear at the landward portion of Essaouira, in an area defined by the culmination of the basement-involved and salt-influenced NW-SE high that probably formed by reactivation of the syn-rift TAZ (Figs. 10–11 and 18) and is regarded as the offshore continuation of the Atlas Fold-Belt (Hafid et al., 2000, 2006; Tari et al., 2017). These Senonian sheets have more complex geometries than the earlier, Albian-Cenomanian ones, being drastically thinned and associated with sets of updip basinward-dipping normal faults (roho) that indicate greater downdip salt evacuation and gliding (Figs. 10 and 11).

6.3. BTU-Paleogene

The third generation of allochthonous salt is associated with the regional expression of the major erosional BTU unconformity (Tari and Jabour, 2013) and coincides with the peak of thick-skinned contraction along the margin (Fig. 18c). Contraction continued to propagate offshore and by this time was affecting the entire salt basin (Fig. 17). This resulted in the largest volume of salt being extruded over/near this regional unconformity and development of the largest and thickest canopy systems, which formed by the coalescence of smaller sheets from Senonian to Paleogene times (Fig. 9). These sheets acted as bathymetric highs that, under low sediment input conditions typical of uplifted areas, were not deeply buried and, therefore, were able to advance over thin syn-kinematic sediments and to merge with other sheets basinward (Fig. 18). Most of the allochthonous salt in Safi was already emplaced and their feeders exhausted by the end of Cretaceous due to contraction at the downdip end of the basin, so no new allochthons developed.

6.4. Oligo-Miocene

The final generation of allochthonous salt occurred over the downdip edge of the salt basin and further south at the transition to the Agadir segment (Fig. 18d), represented by smaller (1–3 km wide) salt tongues at the crest of sub-vertical diapirs (Fig. 7). These features appear to have formed by renewed pulses of contraction during the Oligo-Miocene, being highly inflated (1.5–2.5 km thick) and associated with frontal thrusts and uplift of pre-kinematic roofs, suggesting they formed by thrusting rather than extrusion (c.f. Dooley et al., 2015).

6.5. Mechanisms

The earliest generation of allochthonous salt in the Safi segment is explained by more abrupt gliding caused by the steeper and narrower salt detachment and presence of large downdip pre-salt barriers (e.g. volcanoes) enhancing contraction (Figs. 14–16). The occurrence of Late Cretaceous sheets over the zone of uplifted basement at the updip portion of Essaouira suggests that the offshore continuation of a thick-skinned fold-belt acted as the main control on their generation, favouring diapir squeezing, salt extrusion and enhancing downdip gliding (Figs. 10 and 11). The next and most expressive generation of allochthonous salt occurred further basinward associated with a major erosive event (i.e. BTU, Tari and Jabour, 2013) and propagation of basement-involved contraction, resulting in larger volumes of salt reaching the surface (Figs. 7–9). Generation of allochthonous salt continued to propagate basin- and southward of the thick-skinned fold-belt with thrusting of salt tongues in the Oligo-Miocene (Fig. 7).

Salt sheets formed mainly by salt extrusion near or on the paleo sea-floor, commonly associated with major hiatuses and/or regional erosional events (e.g. Hudec and Jackson, 2006) (Figs. 7 and 10-13). Later Oligo-Miocene salt tongues seem to have involved thrust-piercement (c.f. Hudec and Jackson, 2007), as they are usually narrower, highly-inflated and offset a thin (200–300 m) pre-kinematic roof (Figs. 7–8). The main mechanism of emplacement of allochthonous sheets is, therefore, contraction of sub-vertical feeders (Fig. 19a) related to both gravity and thick-skinned tectonics. In both cases, hangingwall strata are generally thinner and uplifted relative to the downdip footwall (Figs. 11–13, 15 and 19a), occasionally showing fold geometries suggesting reverse shearing/faulting (Figs. 7–8, 11 and 15) (Shaw et al., 2005).

The second mechanism is associated with landward-dipping feeders in which the updip minibasin subsides relative to the downdip one, being commonly associated with basinward-thickening expulsion or extensional rollovers (Figs. 7, 13a and 19b). In this mechanism, an earlier salt ridge that may or may not be associated with a listric landward-dipping normal fault forms a sea-floor topographic barrier that results in ponding of deep-water sediments (Fig. 19b). This produces loading that gradually expels salt seawards, generating seaward-leaning diapirs and basinward-thickening folded strata defining an expulsion rollover (c.f. Ge et al., 1997; Krézsek et al., 2007) (Fig. 18b). This style of growth predominates in the Essaouira segment and, interestingly, occurs in its mid-slope portion, alternating with contraction-driven structures on both sides (Fig. 7).

7. Discussion

7.1. Influence of base-salt relief on allochthonous salt flow

Recent physical (Dooley et al., 2016; Dooley and Hudec 2016; Ferrer et al., 2017) and numerical (Pichel et al., 2018a,b) modelling has shown how pre-salt structures and base-salt relief act as important controls on salt tectonics by promoting flux variations that result in more intricate distribution of structural styles (Fig. 20). Salt and overburden translation over pre-salt horsts results in initial inflation and contraction at their updip edges (landward-dipping base-salt ramps); and later extensional collapse as the salt gradually thickens and accelerates over the horst (base-salt flats, Fig. 20a). Conversely, translation over their downdip edges (basinward-dipping base-salt ramps) produces a zone of salt subsidence limited updip by extension at the top and contraction at the bottom of the ramp (Fig. 20a) (Dooley et al., 2016, 2018; Pichel et al., 2018a; b).

In the case of tilted blocks, salt flux variations, multiphase diapirism and alternation of structural styles are even more pronounced, resulting in pairs of extensional-contractional zones (Fig. 20b and c). These zones have varying widths and deformation magnitudes according to their development over steep or gentle base-salt ramps defined respectively by pre-salt faults and footwalls (Pichel et al., 2018b). Although these models do not include syn-kinematic sedimentation, landward-thickening minibasins (i.e. ramp-syncline basins, Jackson and Hudec, 2005) are expected to develop in these settings above or downdip of base-salt ramps given that aggradation rates are lower than translation rates (RSBs, c.f. Pichel et al., 2018a; Dooley et al., 2018).

A series of RSBs and pairs of extension-contraction zones were identified over allochthonous sheets in a level with higher seismic resolution (Figs. 7, 8 and 10–13), demonstrating evidence of salt and overburden translation (i.e. gliding) over complex base-salt relief. Gliding generated basinward-dipping listric normal faults and extensional rollovers at the rear of salt sheets and near the top of basinward-dipping ramps at their base (Figs. 7, 8, 12 and 13). Immediately downdip, intermediate zones of translation were commonly characterized by landward-dipping gently-folded and sigmoidal growth strata (RSBs) directly onlapping the top allochthonous salt without any direct evidence of faulting (Figs. 7, 8, 12 and 13). These RSBs were defined by basinward-dipping axial traces and finished updip immediately above the top of base-salt ramps (Figs. 7, 8, 10, 12 and 13). Downdip of the RSBs, gliding was accommodated by salt inflation, overburden contraction and uplift, and occasionally, early-stage open-toe advance when the salt sheet frontal edge advanced without roof sediments to record contraction (Figs. 5 and 8). Similar patterns of allochthonous salt flow and complex distribution of supra-salt structural styles have been recently modelled by Dooley et al. (2018) and explained by the interplay between dynamic salt budget and variations of base-salt relief associated with coalescence of sheets.

Although recently recognized in the Gulf of Mexico (Peel, 2018; pers. comm), and briefly described in Pichel et al. (2018a), allochthonous salt-detached RSBs have never been analysed in detail. As shown by novel numerical models (Pichel et al., 2018a), translation results in salt subsidence and syn-kinematic deposition above the base-salt ramp; and as the system evolves, strata move out of the locus of subsidence being rotated and uplifted while new sediments are deposited over the ramp (Figs. 10–13). Where RSBs form, they impose additional loading onto the salt and are, therefore, commonly associated with coeval expulsion below them and inflation downdip.

At the allochthonous salt level, these RSBs typically develop over and/or near sub-vertical squeezed feeders, being highly rotated, asymmetric and with abrupt onlaps towards the top salt (Figs. 8, 10, 12 and 13). This indicates relatively fast flow and subsidence rates that can be attributed to an initially higher salt budget above feeders (c.f. Dooley et al., 2018). Once the feeders are exhausted due to shortening and/or loading, the salt supply is reduced and continuous subsidence and loading within the RSBs tend to expel the underlying salt seaward, thinning the salt above the feeders (Figs. 8, 9c and 12-13). In places, growth strata onlap a drastically thinned/welded landward-dipping segment of the allochthonous sheet indicating more extreme and fast translation over the feeders (Figs. 12 and 13). The distance of the oldest, basinwardmost onlap within the RSBs to the top of their respective base-salt ramp indicates 5–10 km of downdip gliding at the allochthonous level during the Paleogene-Miocene, at an approximate rate of 0.2 mm/year (0.2 km/Ma). Translation of salt and overburden may have still occurred without the development of RSBs in areas without base-salt ramps or when the rates of translation relative to

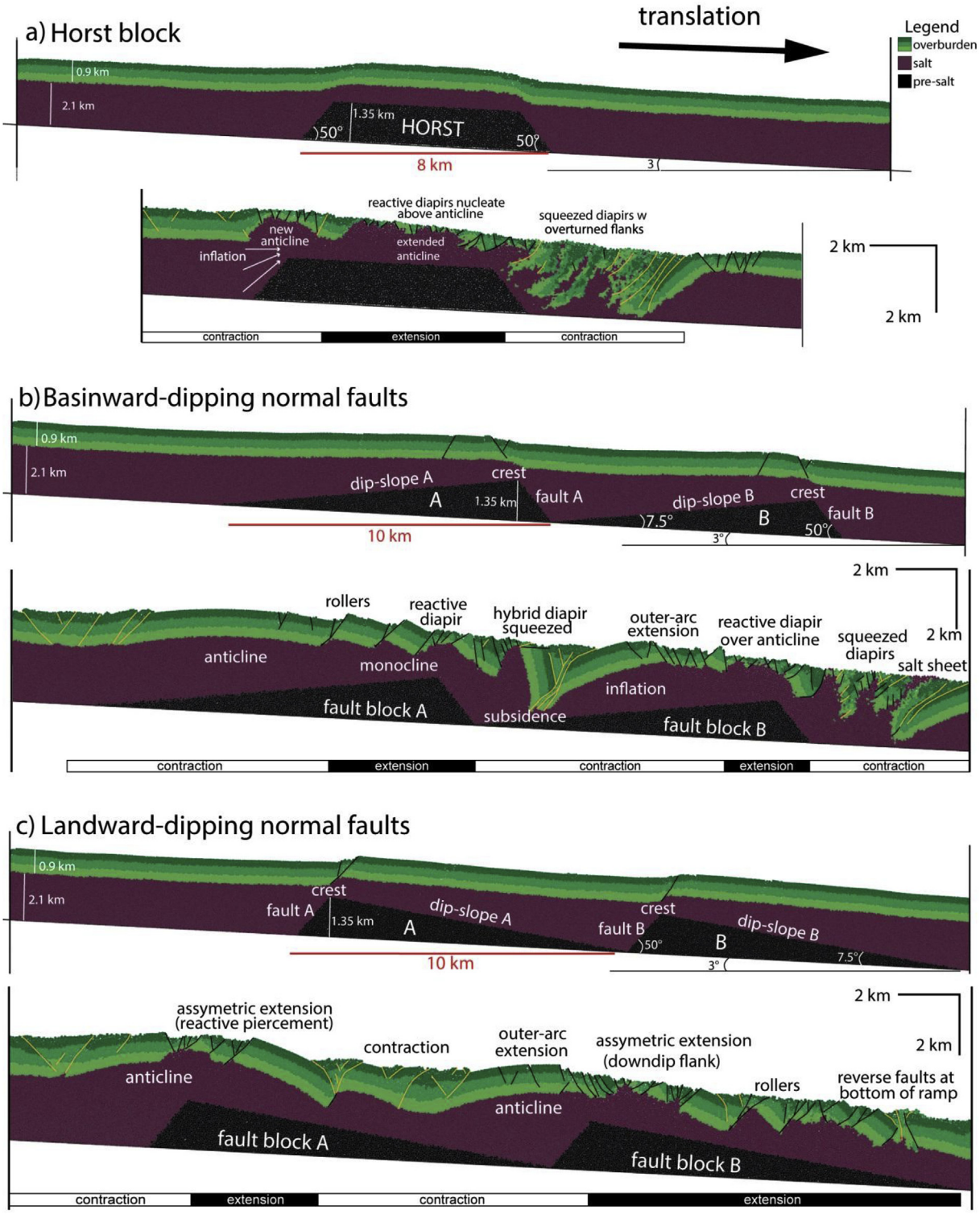

Fig. 20. Discrete-Element models simulating early-stage gliding over pre-salt structures and equivalent base-salt ramps: (a) horst block, (b) tilted fault-blocks defined by basinward-dipping normal faults and in (c) tilted blocks defined by landward-dipping faults (adapted from Pichel et al., 2018b).

sedimentation were low or the sedimentation controlled by a prograding sedimentary wedge (Pichel et al., 2018a).

7.2. Influence of pre-salt rift structures on regional salt tectonics

The relationships described above for allochthonous salt can be used as a proxy to understand the complex sub-salt structural variation and multiphase growth associated with counter-regional feeders observed in the seismic data (Figs. 7, 8 and 10–13). As the salt was deposited during the late syn-rift stage (Tari et al., 2003, 2012), original salt thicknesses are expected to vary dramatically across and within half-grabens (Rowan, 2014; Jackson and Hudec, 2017). As a consequence, early flow must have been largely influenced by pre-salt rift structures and associated flux variations as shown by numerical (Figs. 20 and 21) and physical models (Dooley et al., 2016, 2018).

The effects of syn-rift salt deposition and thickness variations on

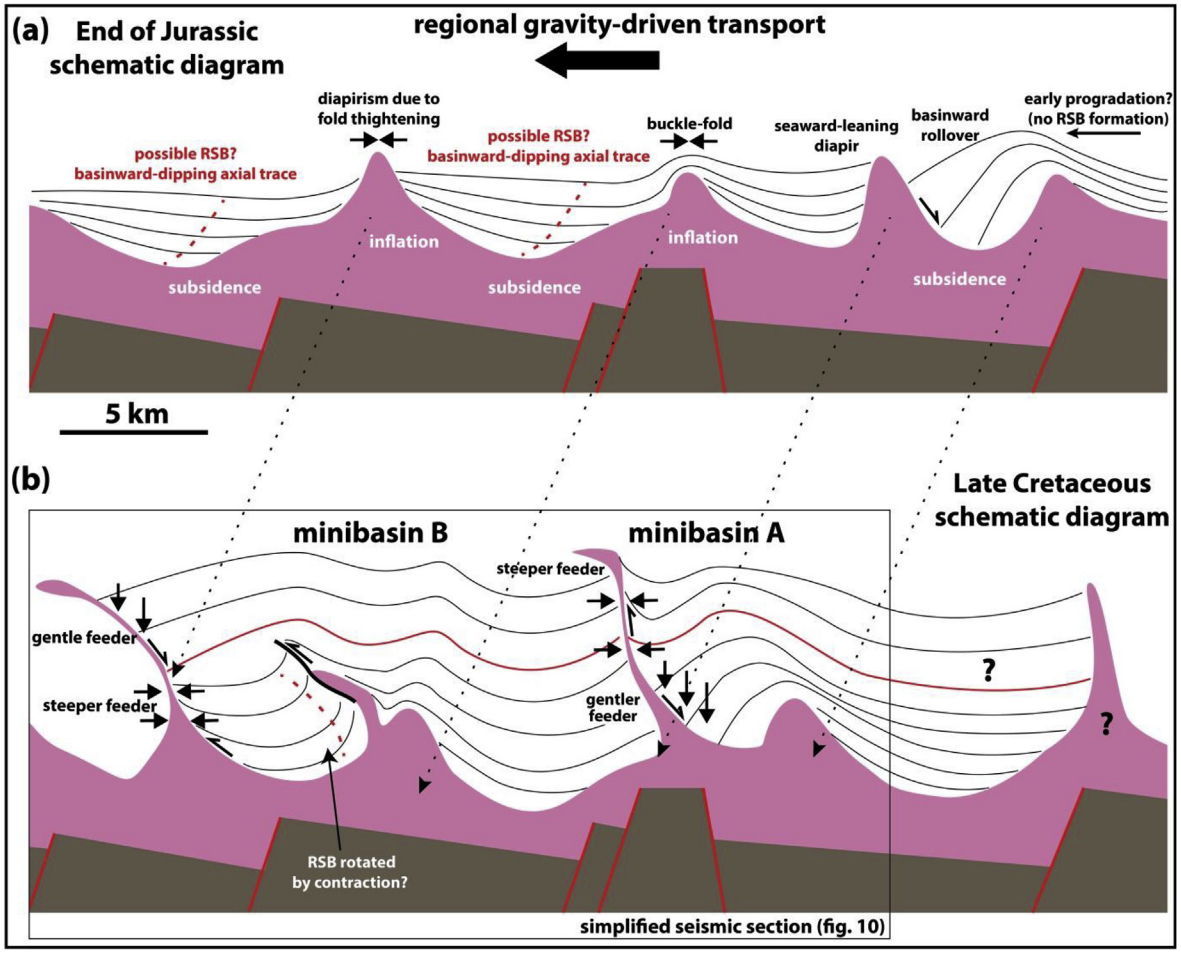

Fig. 21. Simplified kinematic model demonstrating the evolution associated with downdip translation of salt and overburden across complex pre-salt rift topography in the Essaouira segment (compare to the seismic section on Fig. 10). (a) Translation and associated flux mismatches caused by base-salt relief during the Jurassic resulted in subsidence over base-salt lows and salt inflation and contraction over pre-salt highs (horst and crests of tilted fault-blocks). Subsidence favoured the accumulation of prograding sedimentary wedges in more proximal areas and promoted the development of RSBs in more distal areas where the sedimentation rate was lower. (b) Continued translation during the Cretaceous caused early-formed structures to be inverted. Areas of early subsidence were affected by contraction, reverse shearing and uplift over pre-salt highs (minibasin A) and areas of early contraction subsided over pre-salt lows (minibasin B). Subsidence resulted in gently-dipping squeezed feeders due to differential sub-vertical loading and contraction in steep to sub-vertical feeders due to lateral displacement loading.

detachment connectivity and translation offshore Morocco were first described by Tari et al. (2003) who recognized that translation and salt detachment connectivity were higher in areas of initially thicker salt. Along Essaouira, gliding occurred during the Jurassic-Lower Cretaceous, and possibly Cenomanian, producing the larger salt nappe (c. 15–20 km, Figs. 7–8) and greater magnitude of frontal advance than elsewhere along the margin. The largest volume of allochthonous salt and salt structures occurs in this central segment, which is also the widest (Figs. 3 and 7-8). The evidence suggests that the salt was originally thicker and better connected across multiple grabens in the central portion of the basin, where subsidence is expected to be higher. The greater salt thickness and magnitude of downdip translation in this segment resulted in the highest complexity and variable distribution of structural styles along the margin (Figs. 7–13 and 21). The presence of a kinematically-linked system of updip extension, translation and downdip contraction in Safi indicates that gliding was also significant across this segment, but occurred over a narrower (c. 40 km) and simpler salt basin affected by fewer pre-salt rift structures (Fig. 15). Despite the small present-day volume of salt structures implying originally thinner salt and limited connectivity relative to Essaouira, gliding in Safi was aided by the greater steepness of the salt detachment (Figs. 14–16).

In Essaouira, areas of extension and salt expulsion alternate with areas characterized by overburden uplift and reverse shearing (Figs. 7, 8, 10 and 21). Minibasins and their associated feeders show evidence of multiphase growth with early basinward-thickening and subsidence followed by later stratal thinning, upturning and uplift recording an inversion (minibasin A, Figs. 10 and 21). Adjacent minibasins exhibit the opposite history, with earlier stratal thinning, reverse shearing and contraction followed by later basinward-thickening and subsidence (minibasin B, Figs. 10–21). These multiphase evolution patterns are comparable to models simulating downdip gliding over pre-salt horsts and tilted fault-blocks (Figs. 20 and 21), showing that despite the typically limited imaging of the pre-salt interval, the recognition of these complex salt-related styles can aid identification of pre-salt structures (Figs. 10–13).

According to the models, salt subsidence and cover extension occur above basinward-dipping normal faults where salt is initially thicker (Fig. 20b). Contraction and uplift occur as salt flow is buttressed and salt inflates over landward-dipping faults and/or over the dip-slopes of basinward-dipping faults (Fig. 20b and c). We can, then, infer that the updip minibasin (A, Fig. 21) and associated Jurassic rollover originated above a pre-salt low defined by a basinward-dipping normal fault and, as it translated downdip over a pre-salt high, was inverted and uplifted during the Cretaceous. The Jurassic contractional structures of minibasin B formed over this pre-salt high due to early salt inflation and

folding (Fig. 21a), being further contracted as they moved downdip over the dip-slope of a tilted fault-block defined by a basinward-dipping normal fault (Fig. 21b). Further downdip, Cretaceous strata of mini-basin B subsided and thickened basinward above an area of thick salt over this basinward-dipping normal fault (Fig. 21b). This multiphase evolution is also recorded by the present-day geometry of squeezed feeders, which dip gently due to increased vertical load when associated with subsidence and basinward-thickening strata; and steeply due to displacement loading related to shortening and diapir squeezing (Fig. 21b).

The observed alternation of growth patterns associated with sub-vertical feeders and diapirs in Essaouira (Figs. 7, 8 and 10) and Safi (Figs. 13–15), and the development of RSBs above autochthonous salt attest the impact of pre-salt rift topography on salt tectonics offshore Morocco. Movement over pre-salt relief generated earlier salt structures that acted as weakness zones for later events (i.e. differential loading and regional contraction), favouring the development of large volumes of allochthonous salt sheets. This occurred to a greater extent in Essaouira, where salt thickness and translation were greater (Figs. 7 and 8); demonstrating a positive relationship between translation, salt thickness and supply for allochthonous salt.

7.3. Relationship between sediment input and structural style variations

In addition to the initial salt thickness variation, differences in sediment input have also been suggested to have a significant influence on along-strike structural style contrasts (Tari et al., 2003, 2012; Tari and Jabour, 2013). Expanding on these pioneer studies, we integrate seismic data with recently published numerical forward models to test the effect of sedimentation on the growth of active diapirs (Fig. 22) (Pichel et al., 2017).

The largest contrast in thickness and sedimentation volume occurs within the Cenozoic succession, which is thicker (c. 2–2.2 km) in Agadir and becomes thinner to the south, being c. 1.6–1.7 km and 1–1.1 km thick on average in Essaouira and Safi, respectively (compare Figs. 5, 7 and 13–15). During this period, the main mechanism controlling salt deformation was regional contraction as seen by the widespread occurrence of squeezed diapirs along the entire margin (Figs. 5–8 and 16). Numerical models show the relationship between sediment input and growth style of squeezed diapirs (Fig. 22), producing similar geometries to those observed on the seismic data, especially when comparing them to the end-members scenarios of the thickest and thinnest syn-shortening interval of Agadir (Fig. 5) and Safi (Fig. 15). In these areas, the structural evolution is simpler and the volume of allochthonous salt smaller, allowing more confident analysis of the impact of sedimentation on the growth of diapirs and, consequently, direct comparison with the models.

Where sediment input was higher, deformation was dominated by vertical movement; resulting in up-right squeezed diapirs c. 3–5 km tall (Figs. 5 and 22b). Where sediment input was half as thick, salt structures are shorter (c. 2–3.5 km), more asymmetric and characterized by seaward-leaning salt tongues (Figs. 13–15 and 22a). Thus, models support the earlier hypothesis that late variations in sediment input also acted as a significant control on the along-strike variation of structural style along the margin (Tari et al., 2012; Tari and Jabour, 2013).

8. Conclusions

The Moroccan Atlantic margin contains notoriously complex salt tectonics due to significant variations in basin morphology, the syn-rift nature of the salt, the imprint of oblique thick-skinned tectonics and contrasts in late sedimentation patterns. This work shows that in the central and widest portion of the margin, the larger volume of salt structures, greater translation and more complex kinematics reflect an originally thicker salt and greater connectivity across multiple syn-rift structures. Further south, in Agadir, less translation is observed and salt deformation is dominated by vertical diapirism triggered by early downbuilding, followed by burial and late rejuvenation driven by contraction and aided by the largest sediment input along the margin. The northern segment, Safi, is narrower and has a smaller volume of salt structures, suggesting salt was initially thinner. Translation, nevertheless, still occurred due to the pronounced tilt (up to 10°) at base-salt level, but over a smaller area and number of pre-salt structures resulting in simpler kinematically-linked gravity-driven system.

Allochthonous salt sheets developed at different times along the margin during four main phases from the Albian in Safi to Late Cretaceous, Paleocene to Oligo-Miocene in Essaouira. They become younger south- and basinward due to the combined influence of margin configuration, basement-involved contraction and volume of available salt. Albian sheets formed in Safi mainly by contraction at the downdip end of the salt basin against large pre-salt buffers; whereas Late Cretaceous-Paleocene sheets developed by two main mechanisms:

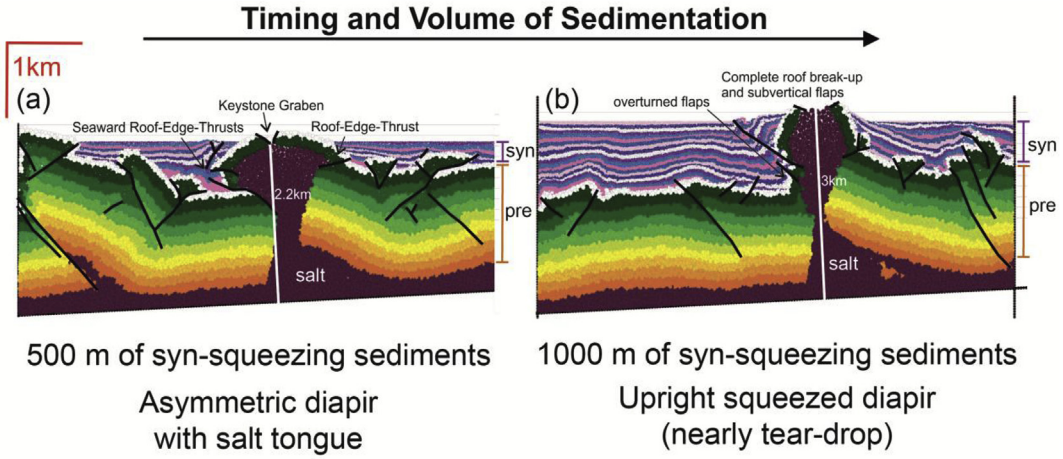

Fig. 22. Discrete-element models simulating rejuvenation of diapirs and syn-kinematic sedimentation testing the effects sediment input on the style of diapir growth (adapted from Pichel et al., 2017). These models are used to explain regional along-strike variation on the style of late diapirism associated with shortening in the margin. (a) Low sediment input (500 m) results in lateral salt advance and development of allochthonous salt sheets such as in Safi where Late Cretaceous-Cenozoic sedimentation was the lowest. (b) High sediment input (1000 m) results in the generation of upright squeezed diapirs such as the ones in Agadir where Late Cretaceous-Cenozoic sedimentation was approximately double that in Safi. Pre- and syn-kinematics sediments are indicated in the model by hot and cold colours and lines at their right-hand side. (For interpretation of the references to colour in this figure legend, the reader is referred to the Web version of this article.)

differential loading and contraction. Distribution of these patterns varies along-dip and strike, with contraction-driven allochthons occurring occasionally updip of expulsion-driven ones, indicating an important control of pre-salt rift topography on salt deformation.

We combined new 3D seismic data and numerical models to demonstrate that the alternation of structural domains and multiphase growth of diapirs and minibasins is caused by pre-salt rift topography and associated variable thickness of syn-rift salt. In Essaouira, where gliding was greater, the variations of supra-salt structural-styles and influence of pre-salt rift topography were also greater than elsewhere. Base-salt relief also influenced flow at the allochthonous level, generating pairs of extensional-contractional zones with intermediate ramp-syncline basins. Despite the often limited resolution of the pre-salt syn-rift intervals, these complex supra-salt geometries can be used to estimate the location of base-salt and rift structures. This is useful for future seismic acquisition, processing and recognition of sub-salt structures, which represent prolific hydrocarbon plays worldwide.

Acknowledgements

The authors would like to thank Chris Jackson, Rob Gawthorpe, Neil Mitchell, Giovanni Bertotti and Andrew Newton for sharing their insights and criticism. We also thank the editor Dario Civile and reviewers Gabor Tari, Ian Davison and Oriol Ferrer for their reviews and constructive criticism that help to improve the quality of this work. We thank ONHYM and Kosmos for allowing us to use their seismic and well data offshore Morocco and especially for access to the 3D seismic data during a two-weeks visit to their headquarters. We also thank William Leslie from Kosmos for reviewing the final version of this manuscript and authorizing its publication. The main author would also like to thank the Science without Borders program and CNPQ, Brazil for sponsoring his PhD research. All authors would also like to thank the NARG sponsors: BP, Repsol, Equinor, Cairn, Woodside, Eni and Total for sponsoring part of this research. Schlumberger is also acknowledged for provision of Petrel software to the University of Manchester.

Appendix A. Supplementary data

Supplementary data to this article can be found online at https://doi.org/10.1016/j.marpetgeo.2019.02.007.

References

Adam, J., Krézsek, C., 2012. Basin-scale salt tectonic processes of the Laurentian Basin, Eastern Canada: insights from integrated regional 2D seismic interpretation and 4D physical experiments. Geol. Soc. Lond. Spec. Publ. 363 (1), 331–360.
Albertz, M., Beaumont, C., Shimeld, J.W., Ings, S.J., Gradmann, S., 2010. An investigation of salt tectonic structural styles in the Scotian Basin, offshore Atlantic Canada: 1. Comparison of observations with geometrically simple numerical models. Tectonics 29 (4).
Brown, A.R., 2011. Interpretation of Three-Dimensional Seismic Data. Society of Exploration Geophysicists and American Association of Petroleum Geologists.
Brun, J.P., Fort, X., 2011. Salt tectonics at passive margins: geology versus models. Mar. Petrol. Geol. 28 (6), 1123–1145.
Davison, I., 2005. Central Atlantic margin basins of North West Africa: geology and hydrocarbon potential (Morocco to Guinea). J. Afr. Earth Sci. 43 (1–3), 254–274.
Davison, I., Anderson, L., Nuttall, P., 2012. Salt deposition, loading and gravity drainage in the Campos and Santos salt basins. Geol. Soc. Lond. Spec. Publ. 363 (1), 159–174.
Deptuck, M.E., Kendell, K.L., 2017. A review of Mesozoic-cenozoic salt tectonics along the Scotian margin, eastern Canada. In: Soto, J.I., Flinch, J., Tari, G. (Eds.), (2017). Permo-Triassic Salt Provinces of Europe, North Africa and the Atlantic Margins: Tectonics and Hydrocarbon Potential. Elsevier, pp. 287–312.
Dooley, T.P., Hudec, M.R., Jackson, M.P., 2012. The structure and evolution of sutures in allochthonous saltSalt Sutures. AAPG Bull. 96 (6), 1045–1070.
Dooley, T.P., Jackson, M.P.A., Hudec, M.R., 2015. Breakout of squeezed stocks: dispersal of roof fragments, source of extrusive salt and interaction with regional thrust faults. Basin Res. 27 (1), 3–25.
Dooley, T.P., Hudec, M.R., Carruthers, D., Jackson, M.P., Luo, G., 2016. The effects of base-salt relief on salt flow and suprasalt deformation patterns—Part 1: flow across simple steps in the base of salt. Interpretation 5 (1), SD1–SD23.
Dooley, T.P., Hudec, M.R., 2016. The effects of base-salt relief on salt flow and suprasalt deformation patterns—Part 2: application to the eastern Gulf of Mexico. Interpretation 5 (1), SD25–SD38.
Dooley, T.P., Hudec, M.R., Pichel, L.M., Jackson, M.P., 2018. The impact of base-salt relief on salt flow and suprasalt deformation patterns at the autochthonous, para-autochthonous and allochthonous level: insights from physical models. Geol. Soc. Lond. Spec. Publ. 476 SP476-13.
Dunlap, D.B., Wood, L.J., Weisenberger, C., Jabour, H., 2010. Seismic geomorphology of offshore Morocco's east margin, Safi Haute Mer area. AAPG Bull. 94 (5), 615–642.
Ferrer, O., Jackson, M.P.A., Roca, E., Rubinat, M., 2012. Evolution of salt structures during extension and inversion of the offshore Parentis Basin (eastern Bay of Biscay). Geol. Soc. Lond. Spec. Publ. 363 (1), 361–380.
Ferrer, O., Gratacós, O., Roca, E., Muñoz, J.A., 2017. Modeling the interaction between presalt seamounts and gravitational failure in salt-bearing passive margins: the Messinian case in the northwestern Mediterranean Basin. Interpretation 5 (1), SD99–SD117.
Frizon de Lamotte, D., Leturmy, P., Missenard, Y., Khomsi, S., Ruiz, G., Saddiqi, O., Guillocheau, F., Michard, A., 2009. Mesozoic and Cenozoic vertical movements in the Atlas system (Algeria, Morocco, Tunisia): an overview. Tectonophysics 475 (1), 9–28.
Ge, H., Jackson, M.P., Vendeville, B.C., 1997. Kinematics and dynamics of salt tectonics driven by progradation. AAPG Bull. 81 (3), 398–423.
Hafid, M., Salem, A.A., Bally, A.W., 2000. The western termination of the Jebilet–high Atlas system (offshore Essaouira Basin, Morocco). Mar. Petrol. Geol. 17 (3), 431–443.
Hafid, M., Zizi, M., Bally, A.W., Salem, A.A., 2006. Structural styles of the western onshore and offshore termination of the High Atlas, Morocco. Compt. Rendus Geosci. 338 (1–2), 50–64.
Hudec, M.R., Jackson, M.P., 2004. Regional restoration across the Kwanza Basin, Angola: salt tectonics triggered by repeated uplift of a metastable passive margin. AAPG Bull. 88 (7), 971–990.
Hudec, M.R., Jackson, M.P., 2006. Advance of allochthonous salt sheets in passive margins and orogens. AAPG Bull. 90 (10), 1535–1564.
Hudec, M.R., Jackson, M.P., 2007. Terra infirma: understanding salt tectonics. Earth Sci. Rev. 82 (1–2), 1–28.
Hudec, M.R., Jackson, M.P., Schultz-Ela, D.D., 2009. The paradox of minibasin subsidence into salt: clues to the evolution of crustal basins. Geol. Soc. Am. Bull. 121 (1–2), 201–221.
Hudec, M.R., Norton, I.O., Jackson, M.P., Peel, F.J., 2013. Jurassic evolution of the Gulf of Mexico salt basin. AAPG Bull. 97 (10), 1683–1710.
Ings, S.J., Shimeld, J.W., 2006. A new conceptual model for the structural evolution of a regional salt detachment on the northeast Scotian margin, offshore eastern Canada. AAPG Bull. 90 (9), 1407–1423.
Jabour, H., Dakki, M., Nahim, M., Charrat, F., El Alji, M., Hssain, M., Oumalch, El Abibi, R., 2004. The Jurassic depositional system of Morocco, geology and play concepts. MAPG Mem 1, 5–39.
Jackson, M.P., Hudec, M.R., 2005. Stratigraphic record of translation down ramps in a passive-margin salt detachment. J. Struct. Geol. 27 (5), 889–911.
Jackson, M.P., Hudec, M.R., 2017. Salt Tectonics: Principles and Practice. Cambridge University Press.
Jackson, C.A.L., Jackson, M.P., Hudec, M.R., 2015a. Understanding the kinematics of salt-bearing passive margins: a critical test of competing hypotheses for the origin of the Albian Gap, Santos Basin, offshore Brazil. Geol. Soc. Am. Bull. 127 (11–12), 1730–1751.
Jackson, C.A.L., Jackson, M.P., Hudec, M.R., Rodriguez, C.R., 2015b. Enigmatic structures within salt walls of the Santos Basin—Part 1: geometry and kinematics from 3D seismic reflection and well data. J. Struct. Geol. 75, 135–162.
Jansa, L.F., Wiedmann, J., 1982. Mesozoic-cenozoic development of the eastern north American and northwest African continental margins: a comparison. In: Geology of the Northwest African Continental Margin. Springer, Berlin, Heidelberg, pp. 215–269.
Jones, I.F., Davison, I., 2014. Seismic imaging in and around salt bodies. Interpretation 2 (4), SL1–SL20.
Krézsek, C., Adam, J., Grujic, D., 2007. Mechanics of fault and expulsion rollover systems developed on passive margins detached on salt: insights from analogue modelling and optical strain monitoring. Geol. Soc. Lond. Spec. Publ. 292 (1), 103–121.
Lancelot, Y., Winterer, E.L., 1980. Evolution of the Moroccan oceanic basin and adjacent continental margin—a synthesis. Initial Rep. Deep Sea Drill. Proj. 50, 801–821.
Luber, T., 2017. Integrated Analysis of Lower Cretaceous Stratigraphy and Depositional Systems: the Essaouira-Agadir Basin of Morocco (Unpublished Doctoral Dissertation). University of Manchester, Manchester, United Kingdom.
Luber, T.L., Bulot, L.G., Redfern, J., Nahim, M., Jeremiah, J., Simmons, M., Bodin, S., Frau, C., Bidgood, M., Masrour, M., 2019. A revised chronostratigraphic framework for the Aptian of the Essaouira-Agadir Basin, a candidate type section for the NW African Atlantic Margin. Cretac. Res. 93, 292–317.
Le Roy, P., Piqué, A., 2001. Triassic–liassic western Moroccan synrift basins in relation to the central Atlantic opening. Mar. Geol. 172 (3–4), 359–381.
McClay, K.R., 1990. Extensional fault systems in sedimentary basins: a review of analogue model studies. Mar. Petrol. Geol. 7 (3), 206–233.
McClay, K.R., 1996. Recent advances in analogue modelling: uses in section interpretation and validation. Geol. Soc. Lond. Spec. Publ. 99 (1), 201–225.
McClay, K., Shaw, J.H., Suppe, J., 2011. Thrust Fault-Related Folding: AAPG Memoir 94, vol. 94 AAPG.
Neumaier, M., Back, S., Littke, R., Kukla, P.A., Schnabel, M., Reichert, C., 2016. Late cretaceous to cenozoic geodynamic evolution of the Atlantic margin offshore Essaouira (Morocco). Basin Res. 28 (5), 712–730.
Peel, F.J., 2014a. How do salt withdrawal minibasins form? Insights from forward modelling, and implications for hydrocarbon migration. Tectonophysics 630, 222–235.
Peel, F.J., 2014b. The engines of gravity-driven movement on passive margins:

quantifying the relative contribution of spreading vs. gravity sliding mechanisms. Tectonophysics 633, 126–142.
Pichel, L.M., Finch, E., Huuse, M., Redfern, J., 2017. The influence of shortening and sedimentation on rejuvenation of salt diapirs: a new Discrete-Element Modelling approach. J. Struct. Geol. 104, 61–79.
Pichel, L.M., Peel, F., Jackson, C.A.-L., Huuse, M., 2018. Geometry and kinematics of salt-detached ramp syncline basins. J. Struct. Geol. 115, 208–230. https://doi.org/10.1016/j.jsg.2018.07.016.
Pichel, L.M., Finch, E., Gawthorpe, R., 2018. The Impact of Pre-salt Rift Topography on Salt Tectonics: a Discrete-Element Modelling Approach.
Quirk, D.G., Schødt, N., Lassen, B., Ings, S.J., Hsu, D., Hirsch, K.K., Von Nicolai, C., 2012. Salt tectonics on passive margins: examples from Santos, Campos and Kwanza basins. Geol. Soc. Lond. Spec. Publ. 363 (1), 207–244.
Roma, M., Ferrer, O., Roca, E., Pla, O., Escosa, F.O., Butillé, M., 2018. Formation and inversion of salt-detached ramp-syncline basins. Results from analog modeling and application to the Columbrets Basin (Western Mediterranean). Tectonophysics 745, 214–228.
Rowan, M.G., Weimer, P., 1998. Salt-sediment interaction, northern Green Canyon and Ewing bank (offshore Louisiana), northern Gulf of Mexico. AAPG Bull. 82 (5), 1055–1082.
Rowan, M.G., Jackson, M.P., Trudgill, B.D., 1999. Salt-related fault families and fault welds in the northern Gulf of Mexico. AAPG Bull. 83 (9), 1454–1484.
Rowan, M.G., Peel, F.J., Vendeville, B.C., 2004. Gravity-driven fold belts on passive margins. In: In: McClay, K.R. (Ed.), Thrust Tectonics and Hydrocarbon Systems, vol. 82. AAPG Memoir, pp. 157–182.
Rowan, M.G., 2014. Passive-margin salt basins: hyperextension, evaporite deposition, and salt tectonics. Basin Res. 26 (1), 154–182.
Rowan, M.G., 2018. The South Atlantic and Gulf of Mexico salt basins: crustal thinning, subsidence and accommodation for salt and presalt strata. Geol. Soc. Lond. Spec. Publ. 476 SP476-6.
Saura, E., Vergés, J., Martín-Martín, J.D., Messager, G., Moragas, M., Razin, P., rélaud, C., Joussiaume, R., Malaval, M., Homke, S., Hunt, D.W., 2014. Syn-to post-rift diapirism and minibasins of the Central High Atlas (Morocco): the changing face of a mountain belt. J. Geol. Soc. 171 (1), 97–105.
Schuster, D.C., 1995. Deformation of allochthonous salt and evolution of related salt-structural systems, eastern Louisiana Gulf Coast. In: In: Jackson, M.P.A., Roberts, D.G., Snelson, S. (Eds.), Salt Tectonics: a Global Perspective, vol. 65. AAPG Memoir, pp. 177–198.
Shaw, J.H., Connors, C.D., Suppe, J., 2005. Seismic Interpretation of Contractional Fault-Related Folds: an AAPG Seismic Atlas, vol. 53 American Association of Petroleum Geologists.
Steiner, C., Hobson, A., Favre, P., Stampfli, G.M., Hernandez, J., 1998. Mesozoic sequence of Fuerteventura (canary Islands): witness of early Jurassic sea-floor spreading in the central Atlantic. Geol. Soc. Am. Bull. 110 (10), 1304–1317.
Tari, G., Molnar, J., Ashton, P., Hedley, R., 2000. Salt tectonics in the Atlantic margin of Morocco. Lead. Edge 19 (10), 1074–1078.
Tari, G., Molnar, J., Ashton, P., 2003. Examples of salt tectonics from West Africa: a comparative approach. Geol. Soc. Lond. Spec. Publ. 207 (1), 85–104.
Tari, G., Molnar, J., 2005. Correlation of syn-rift structures between Morocco and Nova Scotia, Canada. In: Transactions GCSSEPM Foundation, 25th Ann. Res. Conf, pp. 132–150.
Tari, G., Jabour, H., Molnar, J., Valasek, D., Zizi, M., 2012a. Deep-water exploration in Atlantic Morocco: where are the reservoirs? In: Gao, D. (Ed.), Tectonics and Sedimentation: Implications for Petroleum Systems: AAPG Memoir 100, pp. 337–355.
Tari, G., Brown, D., Jabour, H., Hafid, M., Louden, K., Zizi, M., 2012b. The conjugate margins of Morocco and Nova Scotia. In: Regional Geology and Tectonics: Phanerozoic Passive Margins, Cratonic Basins and Global Tectonic Maps, pp. 284–323.
Tari, G., Jabour, H., 2013. Salt tectonics along the Atlantic margin of Morocco. Geol. Soc. Lond. Spec. Publ. 369 (1), 337–353.
Tari, G., Novotny, B., Jabour, H., Hafid, M., 2017. Salt tectonics along the Atlantic margin of NW Africa (Morocco and Mauritania). In: Soto, J.I., Flinch, J., Tari, G. (Eds.), Permo-Triassic Salt Provinces of Europe, North Africa and the Atlantic Margins: Tectonics and Hydrocarbon Potential. Elsevier, pp. 331–351 (2017).
Vendeville, B.C., Jackson, M.P.A., 1992. The fall of diapirs during thin-skinned extension. Mar. Petrol. Geol. 9 (4), 354–371.
Vergés, J., Moragas, M., Martín-Martín, J.D., Saura, E., Casciello, E., Razin, P., Grélaud, C., Malaval, M., Joussiame, R., Messager, G., Sharp, I., 2017. Salt tectonics in the Atlas mountains of Morocco. In: Permo-Triassic Salt Provinces of Europe, North Africa and the Atlantic Margins, pp. 563–579.
Weatherall, P., Marks, K.M., Jakobsson, M., Schmitt, T., Tani, S., Arndt, J.E., et al., 2015. A new digital bathymetric model of the world's oceans. Earth Space Sci. 2 (8), 331–345.